



Spatial In Situ Structural Health Monitoring for Fiber-Reinforced Polymer Composites

SAND2012-4688P

UNIVERSITY OF CALIFORNIA, DAVIS

Bryan R. Loyola

Department of Mechanical & Aerospace Engineering

Advisors:

Valeria La Saponara

Advanced Composites Research, Engineering, and Science (ACRES) Laboratory
Department of Mechanical and Aerospace Engineering

Kenneth J. Loh

Nano-Engineering & Smart Structures Technologies (NESST) Laboratory
Department of Civil and Environmental Engineering

Doctoral Exit Seminar

Department of Mechanical and Aerospace Engineering, UC Davis
June 7, 2012

Presentation Outline

- **Introduction**
 - ❖ Why does structural health monitoring (SHM) for fiber-reinforced polymer (FRP) composites matter?
- **Implementation of carbon nanotubes**
 - ❖ Utilizing their impressive properties for structural monitoring
- **Characterizing nanocomposite sensors**
 - ❖ What are their mechanical sensing capabilities?
- **Changing the SHM paradigm to spatially distributed sensing**
 - ❖ From discrete to distributed sensing using electrical impedance tomography
- **Validating spatial sensing for common FRP damage modes**
 - ❖ How well does multi-modal spatial sensing perform?



Usage of Fiber-Reinforced Composites

- Over the past 50 years, increased usage of composite materials



Commercial aircraft systems



Space shuttle and space structures



Military aircraft



Naval structures



Wind turbine blades



CFRP cable stay bridge



Composite Damage Modes

- **Susceptible to damage due to:**

- ❖ Strain, impact, chemical penetrants, multi-axial fatigue

- **Damage modes:**

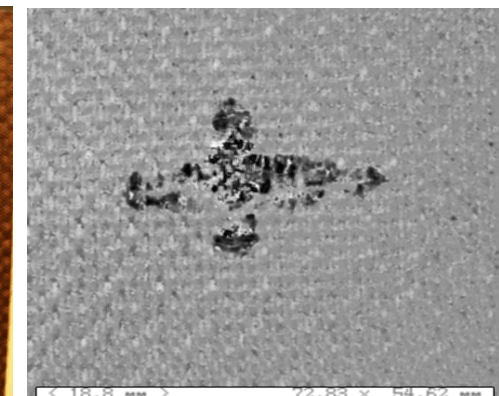
- ❖ Matrix cracking
 - ❖ Fiber-breakage
 - ❖ Delamination
 - ❖ Transverse cracking
 - ❖ Fiber-matrix debonding
 - ❖ Matrix degradation
 - ❖ Blistering

- **Difficult to detect**

- ❖ Internal to laminate structure
 - ❖ Nearly invisible to naked eye

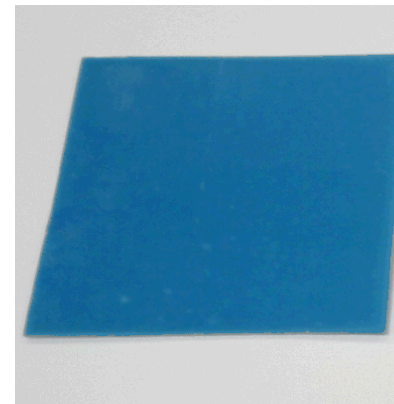


Visual inspection



C-SCAN ultrasound image

CFRP panel after 20 Joule impact



Adhesive exposed to hydraulic fluid at 70°C
Sugita *et al*, (2010)



Emerging Sensing Technologies

Wireless Sensors and Sensor Networks



WiMMS

Wang, *et al.* (2008)

UCI DuraNode

Chung, *et al.* (2005)

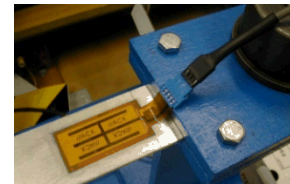
Advantages:

- ❖ Low cost
- ❖ Dense instrumentation
- ❖ Reconfigurable

Disadvantages:

- ❖ Point sensors
- ❖ Indirect damage detection
- ❖ Physics-based models

Ultrasonics and Guided-Waves



Array of piezoelectric ceramic sensors and actuators

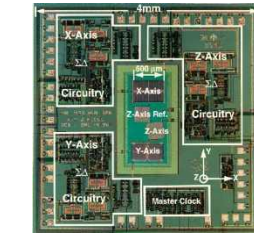
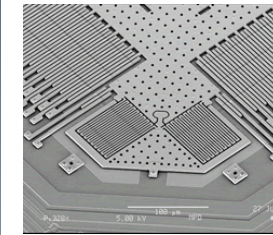
Advantages:

- ❖ Sensors and actuators
- ❖ Spatial damage detection

Disadvantages:

- ❖ Indirect damage detection
- ❖ Wave propagation models or pattern recognition
- ❖ Thin metallic structures
- ❖ Expensive data acquisition

Micro-electromechanical Systems (MEMS)



AD iMEMS

Weinberg (1999)

3-axis accelerometer

Lemkin (1997)

Advantages:

- ❖ Miniaturized sensor designs
- ❖ Complex sensors/actuators

Disadvantages:

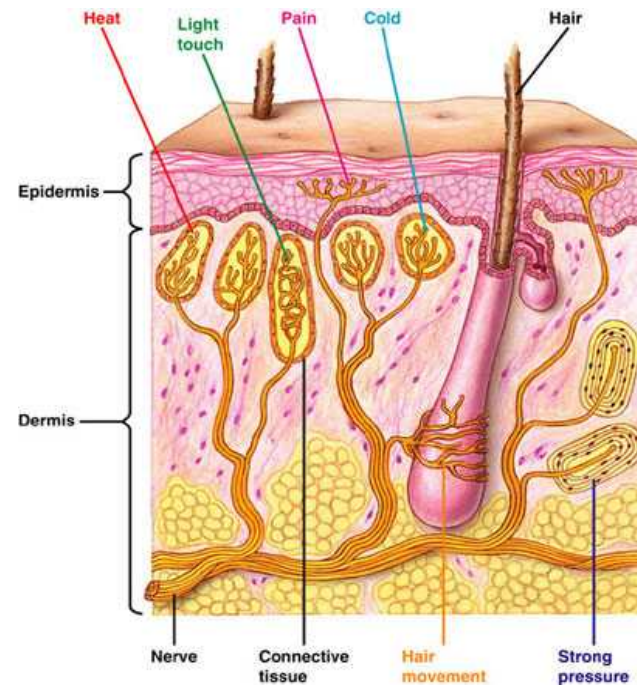
- ❖ “Top-down” design
- ❖ Expensive fabrication equipment
- ❖ High costs
- ❖ Sensor sensitivity on par with macro-scale counterpart



SHM Design Considerations

Current SHM limitations

- ❖ Indirect sensing approaches
- ❖ Point-based sensing
- ❖ Tethered sensors
- ❖ Lack of system scalability



Overview of the human dermatologic system (Mallory 2008)

Successful SHM system

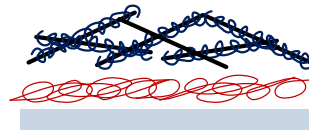
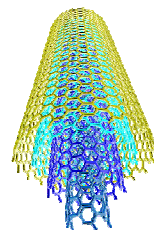
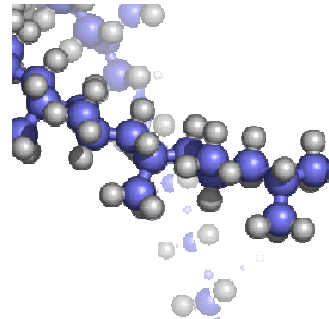
1. Directly detect and measure damage
2. Determine the damage location
3. Ascertain the size of the damage
4. Quantify the severity of the damage
5. Achieve multi-modal sensing capabilities (i.e., delamination, cracking, and chemical penetration)



Presentation Outline

PART I

Development of carbon nanotube-based nanocomposites for multi-modal sensing

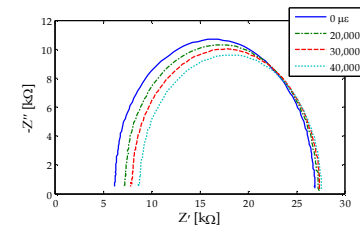


1. Harness unique material properties of carbon nanotubes

2. Layer-by-layer “bottom-up” thin film multi-modal sensor design

PART II

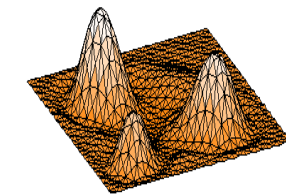
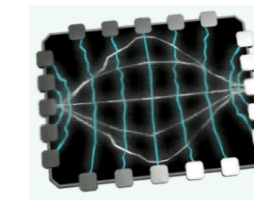
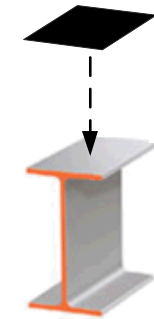
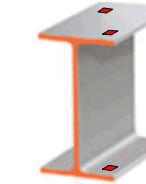
Embedded nanocomposite strain sensors for glass fiber-reinforced polymer composites



3. Deposited thin films on FRP for strain sensing

PART III

From point-sensing to distributed sensing using bio-inspired sensing skins



4. Electrical impedance tomography for spatial conductivity mapping

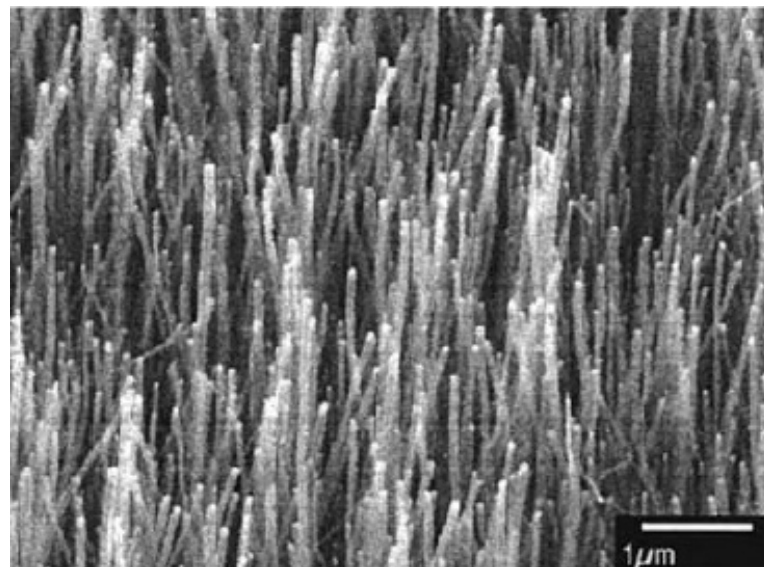
5. Distributed spatial damage sensing based on sensing skins



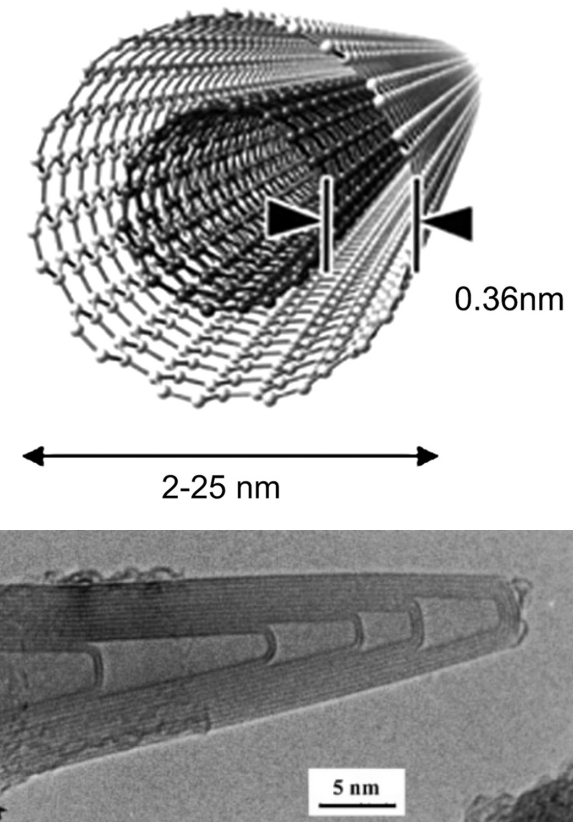
Carbon Nanotubes

Multi-walled carbon nanotubes (MWNT):

- Rolled concentric cylindrical structures constructed of graphene sheets
- Diameter: $6 \sim 100$ nm
- High-aspect ratios: $\sim 10^3$ to 10^7
- Metallic conductivity
- Five times stiffer and ten times stronger than steel



Aligned carbon nanotube forest
Thostenson, et al. (2001)



TEM imagery of an end cap of a MWNT
Harris (2004)



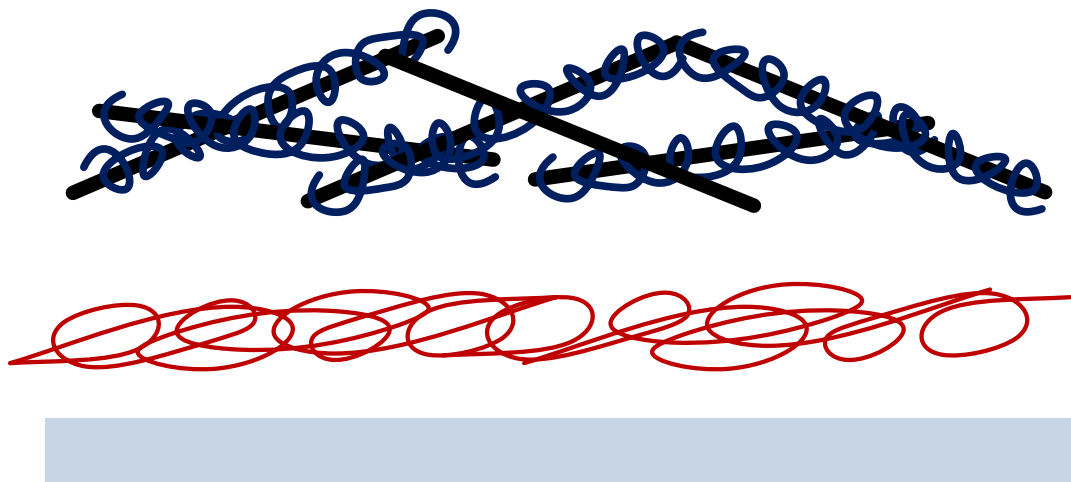
Layer-by-Layer (LbL) Method

- **Sequential assembly of oppositely-charged nanomaterials onto a charged substrate**
 - Bottom-up fabrication methodology
 - Incorporation of a wide variety of nanomaterials
 - 2.5-dimensional nano-structuring to design multifunctional composites
- **Excellent physical, mechanical, and electrical properties:**
 - Physical: homogeneous percolated nano-scale morphology
 - Mechanical: high strength, stiffness, and ductility

2. Negatively-charged monolayer
MWNT-PSS

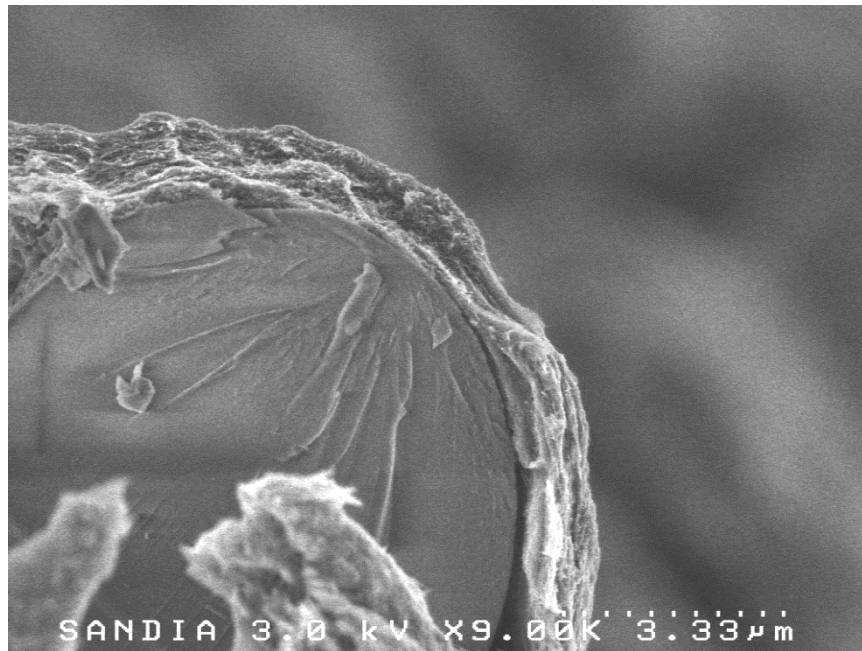
1. Positively-charged monolayer
PVA, PANI, etc.

0. Negatively-charged substrate
GFRP composite

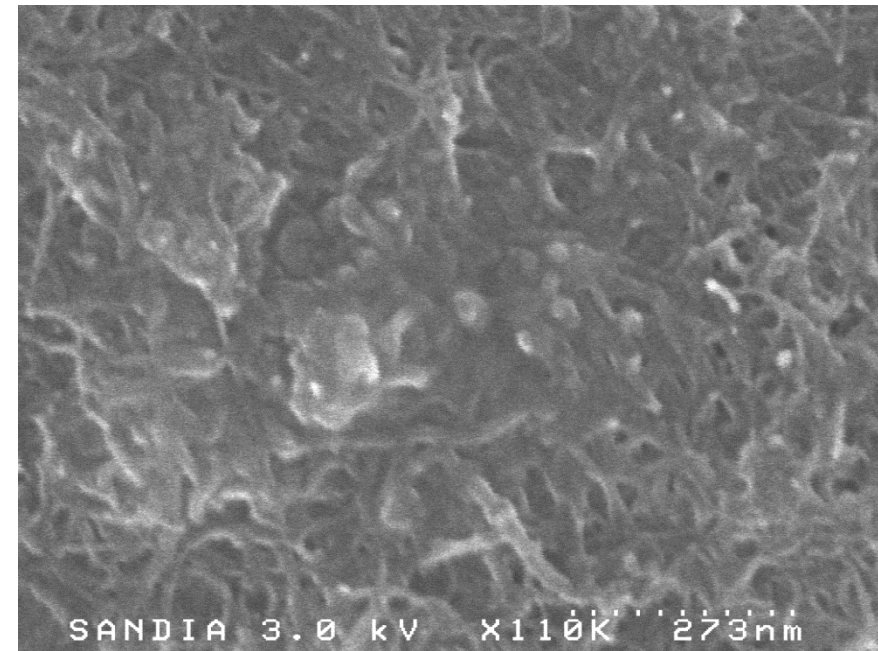


Nanocomposite Morphology

- **Mechanical strength and electrical conductivity/sensing derived from percolated thin film morphology**
 - ❖ Homogeneous composite with similar properties across entire film
 - ❖ Scanning electron microscopy (SEM) imagery to evaluate percolation and uniformity



Scanning electron microscopic (SEM) cross-section view of a 150 bilayer MWNT-PSS/PVA thin film on GFRP



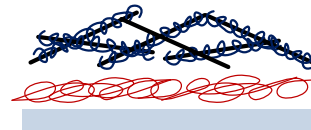
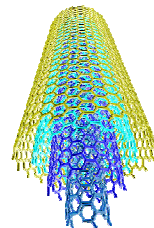
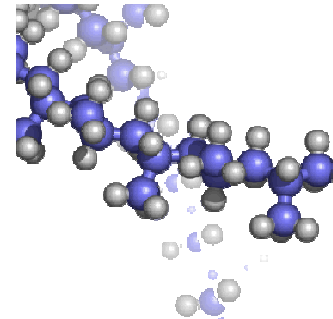
Surface SEM image of a 100 bilayer MWNT-PSS/PVA thin film



Presentation Outline

PART I

Development of carbon nanotube-based nanocomposites for multi-modal sensing

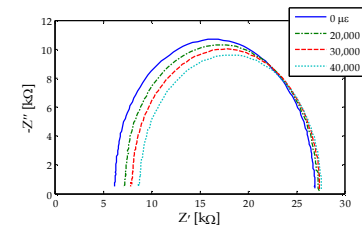


1. Harness unique material properties of carbon nanotubes

2. Layer-by-layer “bottom-up” thin film multi-modal sensor design

PART II

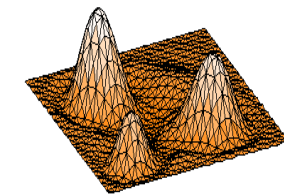
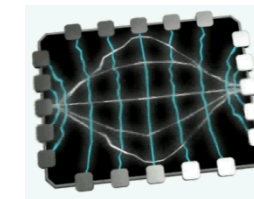
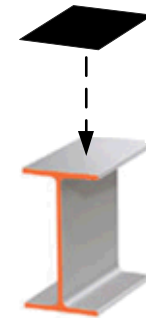
Embedded nanocomposite strain sensors for glass fiber-reinforced polymer composites



3. Deposited thin films on FRP for strain sensing

PART III

From point-sensing to distributed sensing using bio-inspired sensing skins



4. Electrical impedance tomography for spatial conductivity mapping

5. Distributed spatial damage sensing based on sensing skins



Piezoresistivity Validation

Objective:

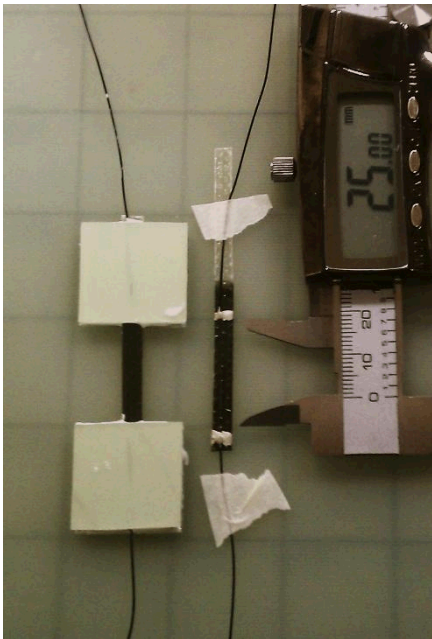
- Validate thin film electromechanical performance deposited on GFRP

Specimen preparation:

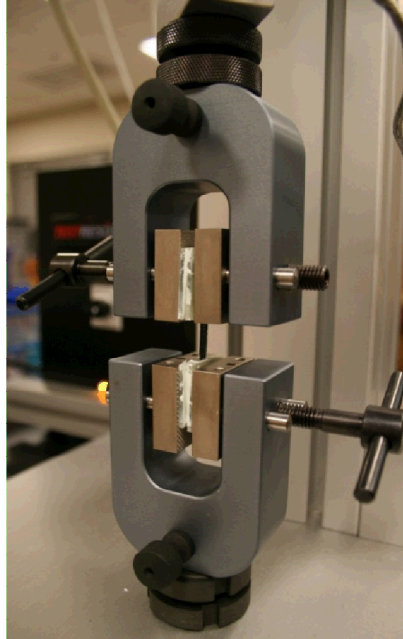
- Attach two conductive electrodes and composite tabs

Nanocomposite electromechanical performance characterization:

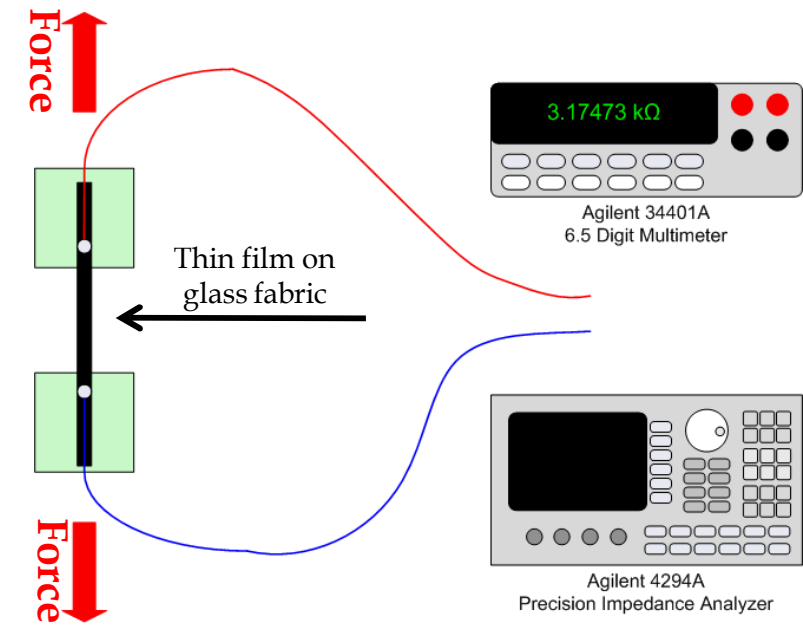
- Apply monotonic and dynamic uni-axial tensile loading to specimens



Fiber-coated specimen



Thin film mounted in load frame



Time- and frequency-domain strain sensing



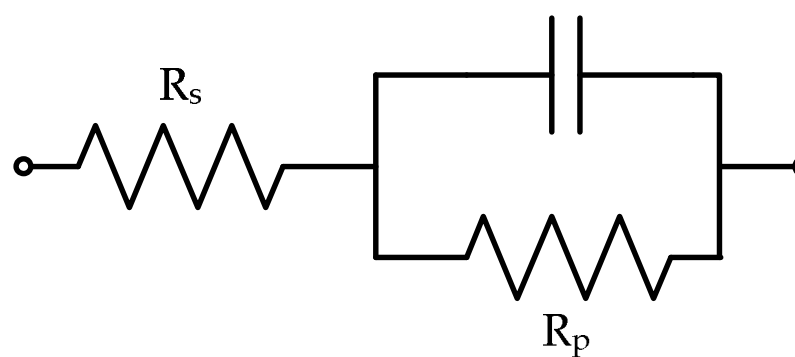
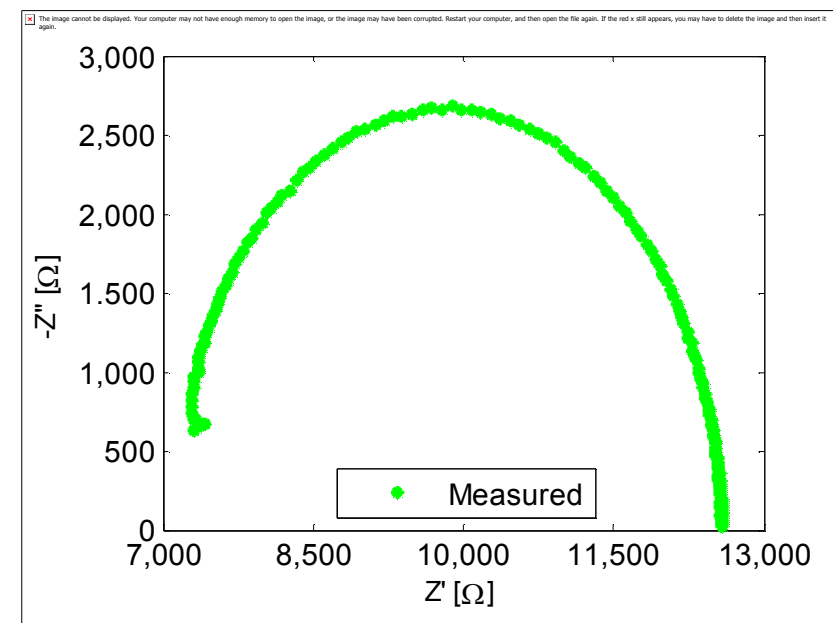
Electrical Impedance Spectroscopy (EIS)

□ Electrical impedance spectroscopy:

- Provides greater insight as compared to bulk resistivity measurements
- Measurement of complex electrical impedance across spectrum of frequencies (40 Hz – 110 MHz)

$$Z(\omega) = \frac{V(j\omega)}{I(j\omega)} = |Z(\omega)| \angle \phi(\omega) = Z'(\omega) + jZ''(\omega)$$

- Physically-based equivalent circuits are used to fit to the impedance data

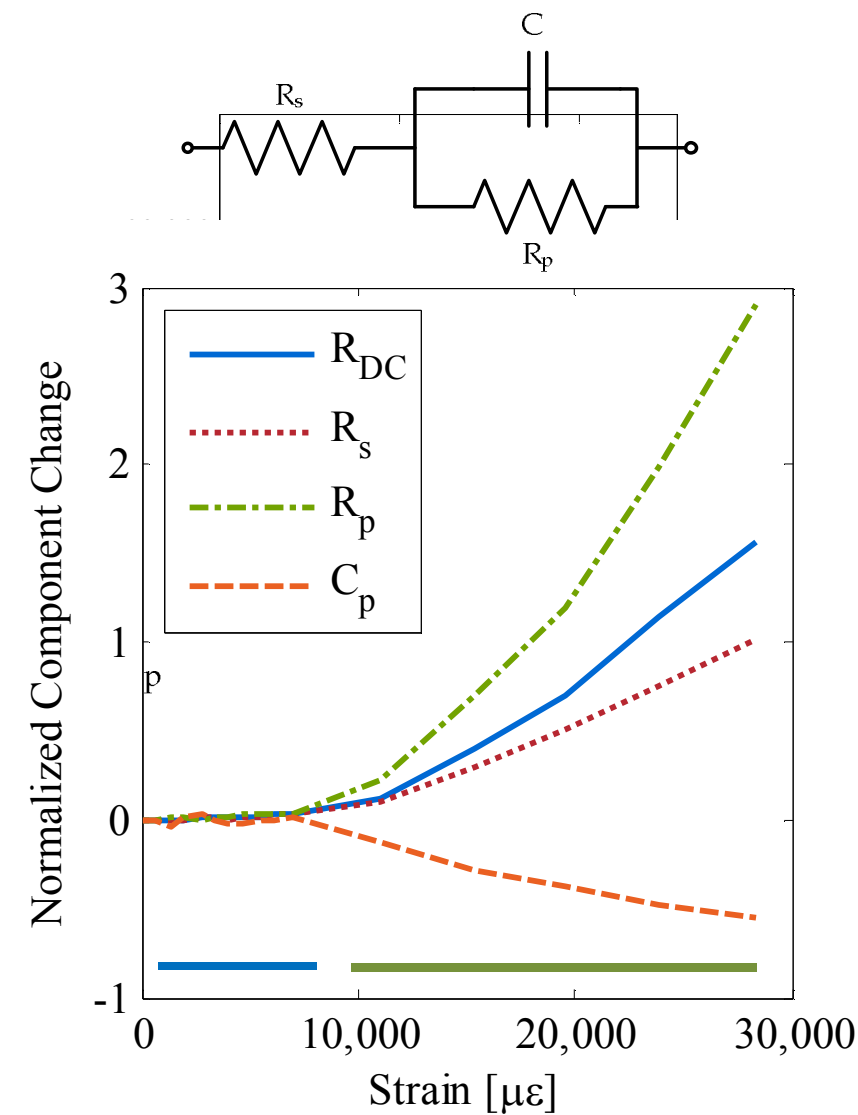


Proposed equivalent circuit model for LbL thin films

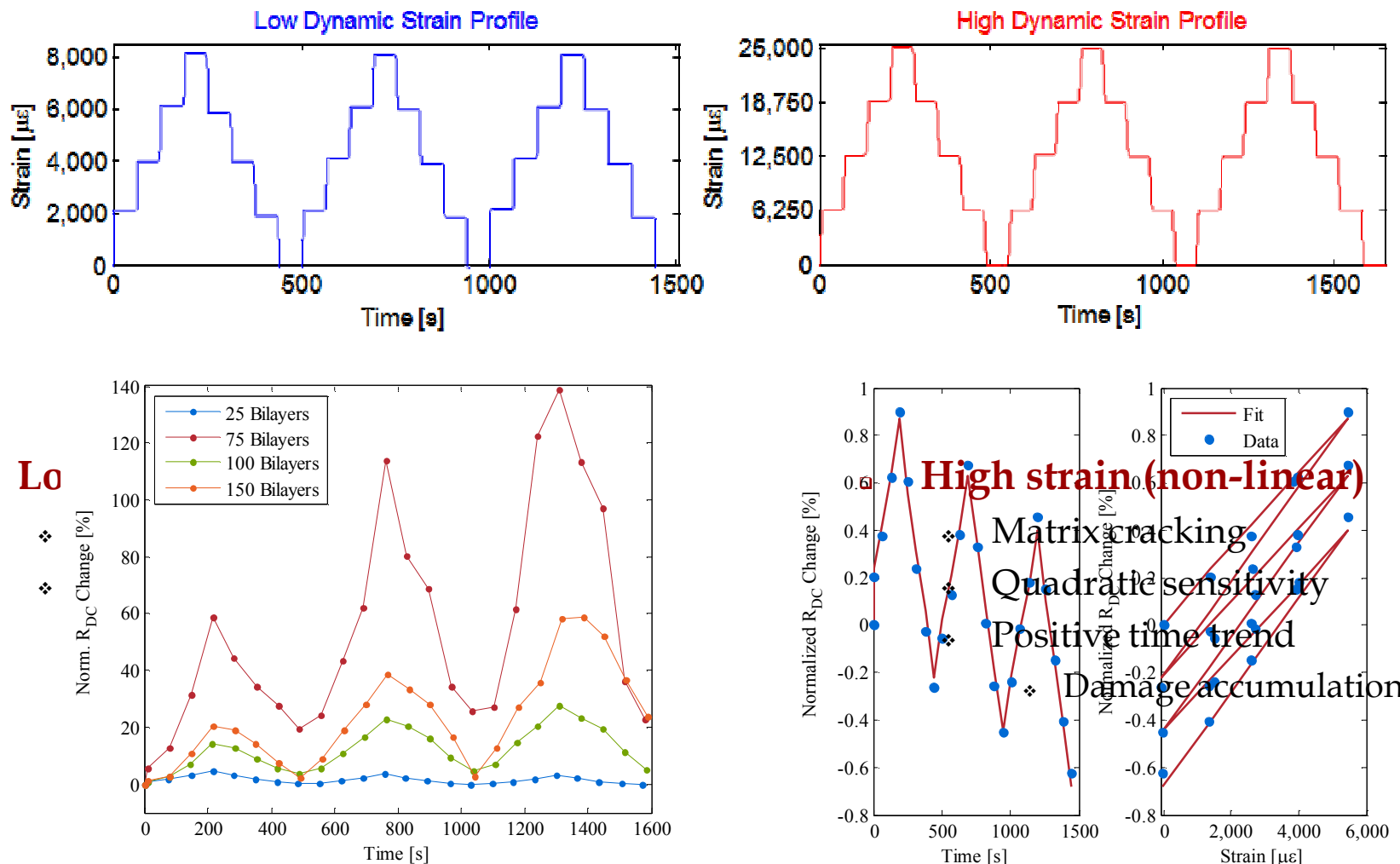


Monotonic Sensor Characterization

- Load frame applies stepped-tensile displacement profile:
 - Monotonic increasing strain to failure
 - Capture full sensors response
- Equivalent circuit model-updating:
 - Fitting with nonlinear least squares
 - Extract fitted circuit parameters as a function of applied strain
- Bi-functional strain sensitivity:
 - Low strain region:
 - Linear response (elastic)
 - High strain region:
 - Quadratic Response
 - Damage to GFRP/thin film



Dynamic Sensor Characterization



Preliminary Results

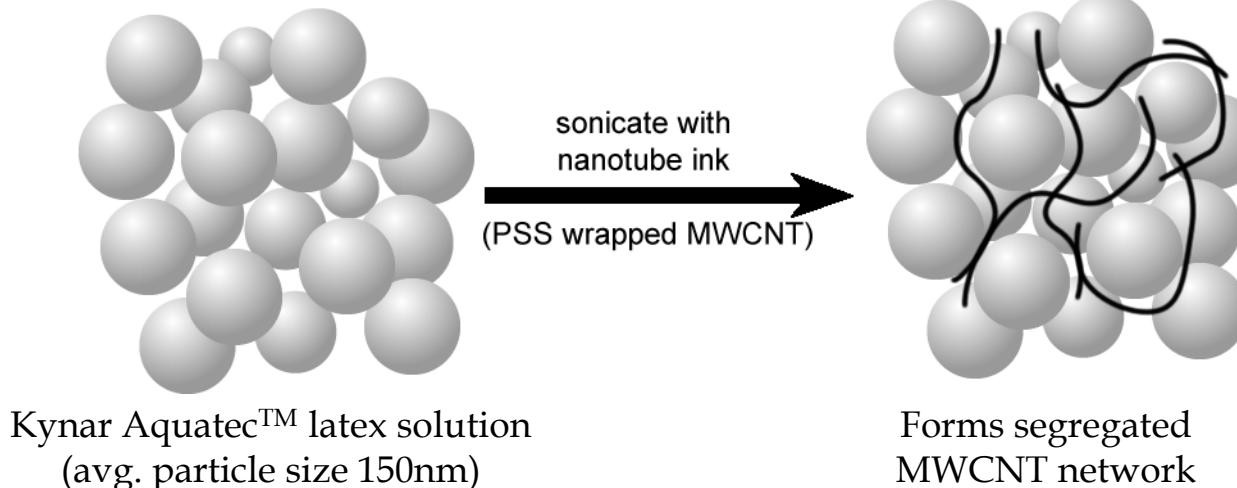
- **Application of a strain sensitive carbon nanotube thin film:**
 - ❖ Layer-by-layer deposition process
 - ❖ Direct deposition on GFRP
 - ❖ Demonstrated piezoresistivity
- **Bi-function strain sensitivity:**
 - ❖ Time and frequency-domain characterization
 - ❖ Demonstrated in monotonic and dynamic loading
 - ❖ Low strain region:
 - ❖ Linear strain sensitivity
 - ❖ High strain region:
 - ❖ Quadratic sensitivity
 - ❖ Damage accumulation
- **Deposition limitations:**
 - ❖ Substrates required to be less than a few square inches in size



Sprayable MWNT-Latex Thin Film

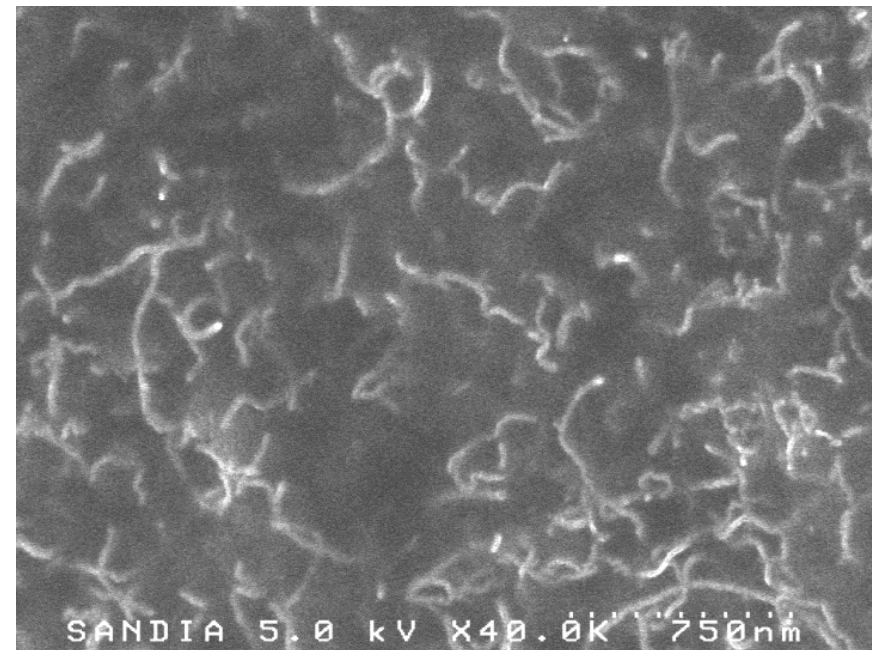
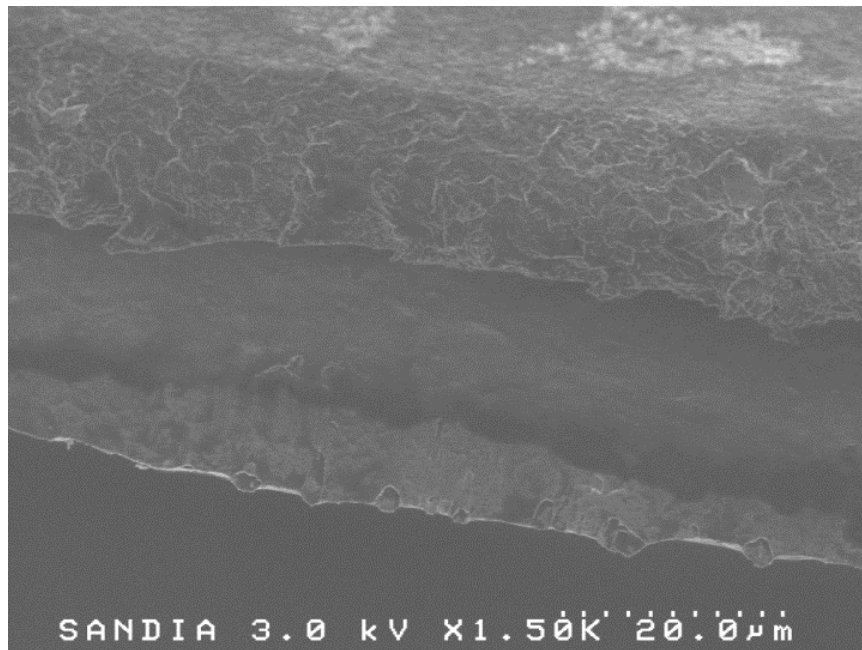
- **Rapid large-scale deposition**
 - ❖ Required for mass deployment of methodology

- **MWNT-PSS/Latex paint formulation**
 - ❖ Collaborated to improve initial Sandia formulation
 - ❖ Sub-micron PVDF creates mold for MWNT organization
 - ❖ Off-the-shelf deposition method



MWNT-Latex Morphology

- **Creation of MWNT networks**
 - ❖ Electrical percolation above 1 wt% MWNTs
- **Fiber-reinforced polymer deployment**
 - ❖ Surface applied to post-cured composites
 - ❖ Applied to fiber weaves for embedded sensing



Cross-section and MWNT network SEM images of 3wt% MWNT-Latex film



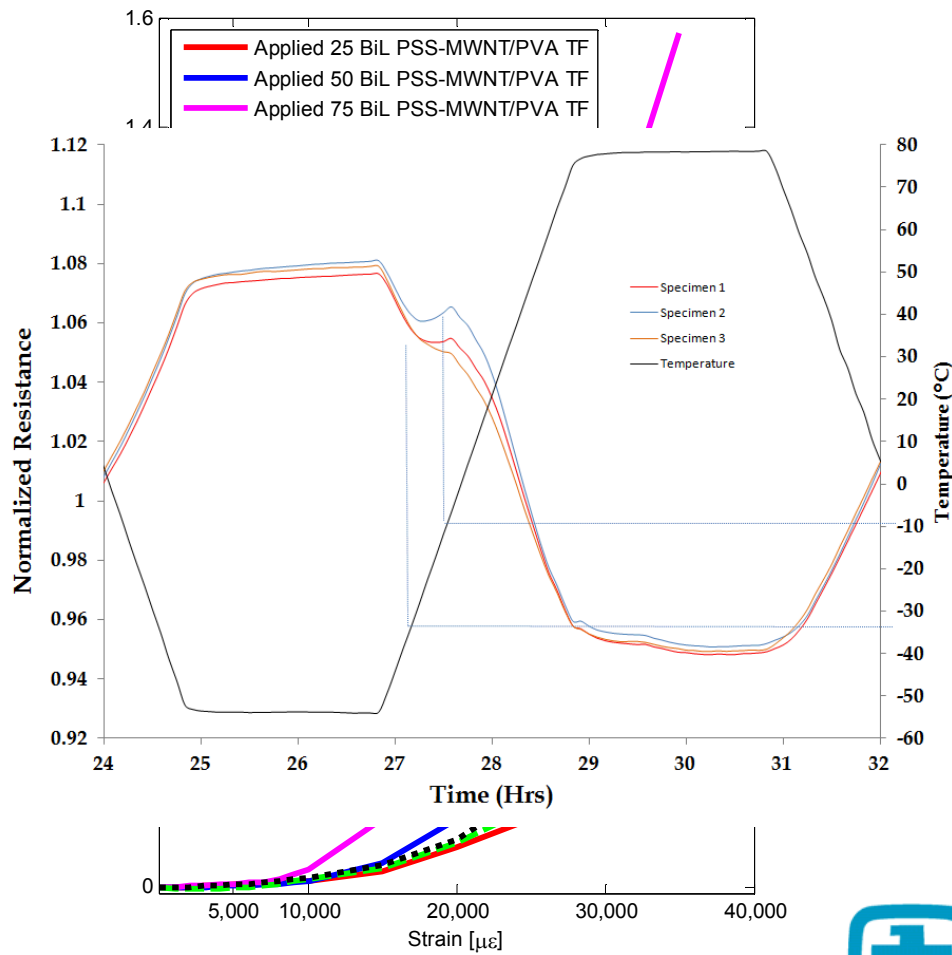
MWNT-Latex Characterization

Electromechanical characteristics

- Quasi-static testing
 - Nearly same sensitivity as LbL
- Bi-functional strain response
 - Linear
 - Quadratic
 - Cracking of film

Thermo-resistance coupling

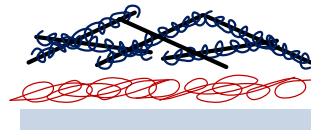
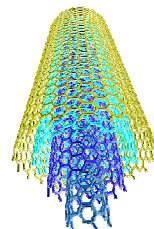
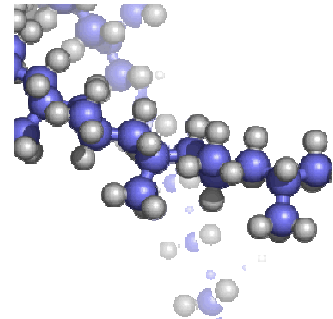
- 50°C to 80°C over 2 hours
- 2 hour holds
- Inversely linear relationship
- Non-linear response @ -30°C
 - $\sim T_g$ of PVDF
 - Restructuring of MWNTs



Presentation Outline

PART I

Development of carbon nanotube-based nanocomposites for multi-modal sensing

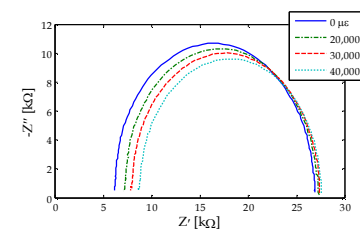


1. Harness unique material properties of carbon nanotubes

2. Layer-by-layer “bottom-up” thin film multi-modal sensor design

PART II

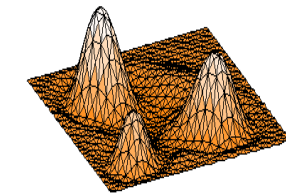
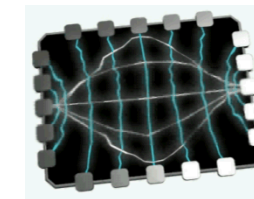
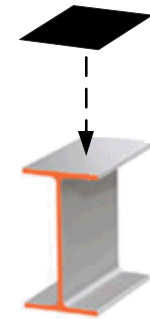
Embedded nanocomposite strain sensors for glass fiber-reinforced polymer composites



3. Deposited thin films on FRP for strain sensing

PART III

From point-sensing to distributed sensing using bio-inspired sensing skins



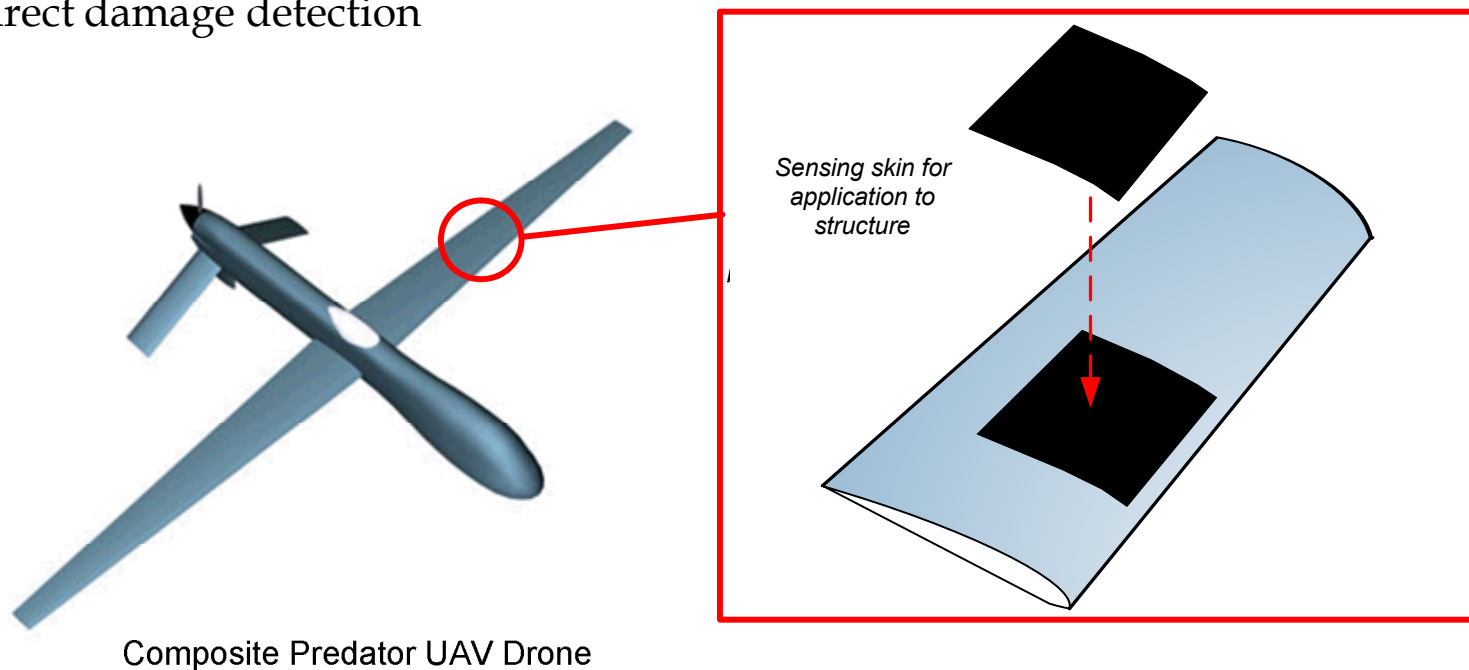
4. Electrical impedance tomography for spatial conductivity mapping

5. Distributed spatial damage sensing based on sensing skins



Spatially Distributed SHM Paradigm

- **Current state-of-art in structural health monitoring:**
 - ❖ Passive SHM using acoustic emissions
 - ❖ Active SHM using piezoelectric sensor/actuator pairs
- **“Sensing skins” for spatial damage detection:**
 - ❖ Objective is to identify the location and severity of damage
 - ❖ Monitor and detect damage over two- (or even three) dimensions
 - ❖ Direct damage detection



Composite Predator UAV Drone

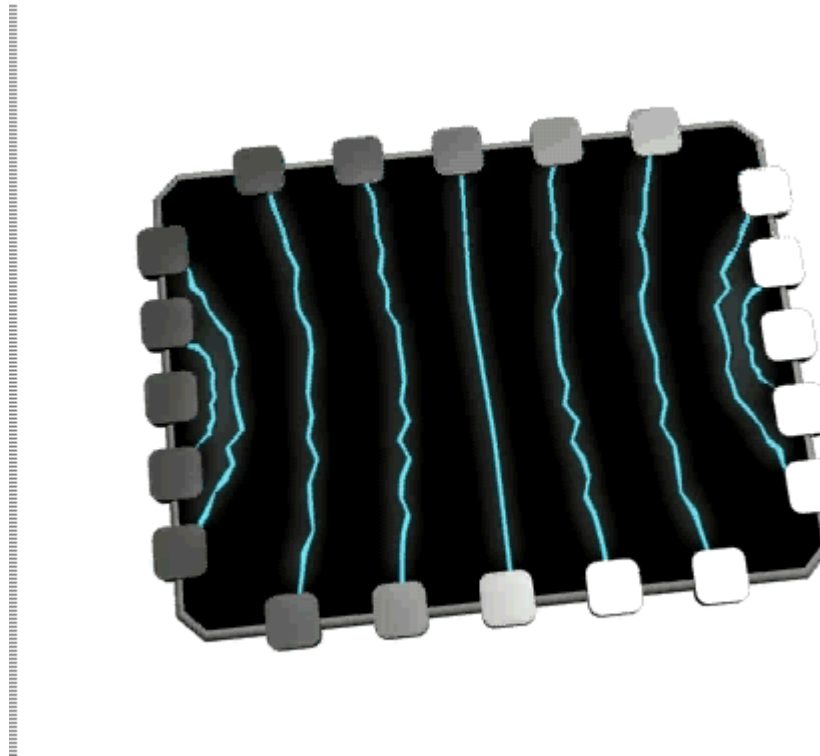
p



Electrical Impedance Tomography

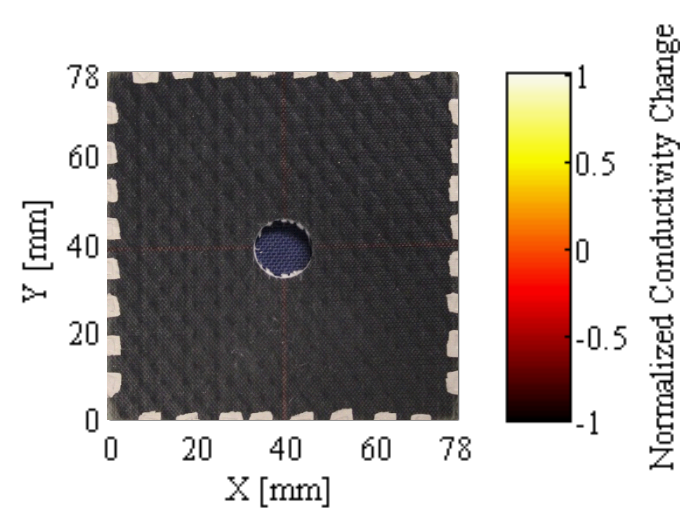
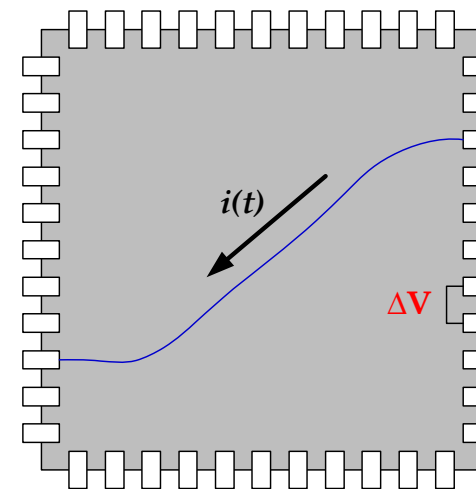
□ Overview of spatial conductivity mapping

- ❖ Since film impedance calibrated to strain, conductivity maps can correspond to 2-D strain distribution maps



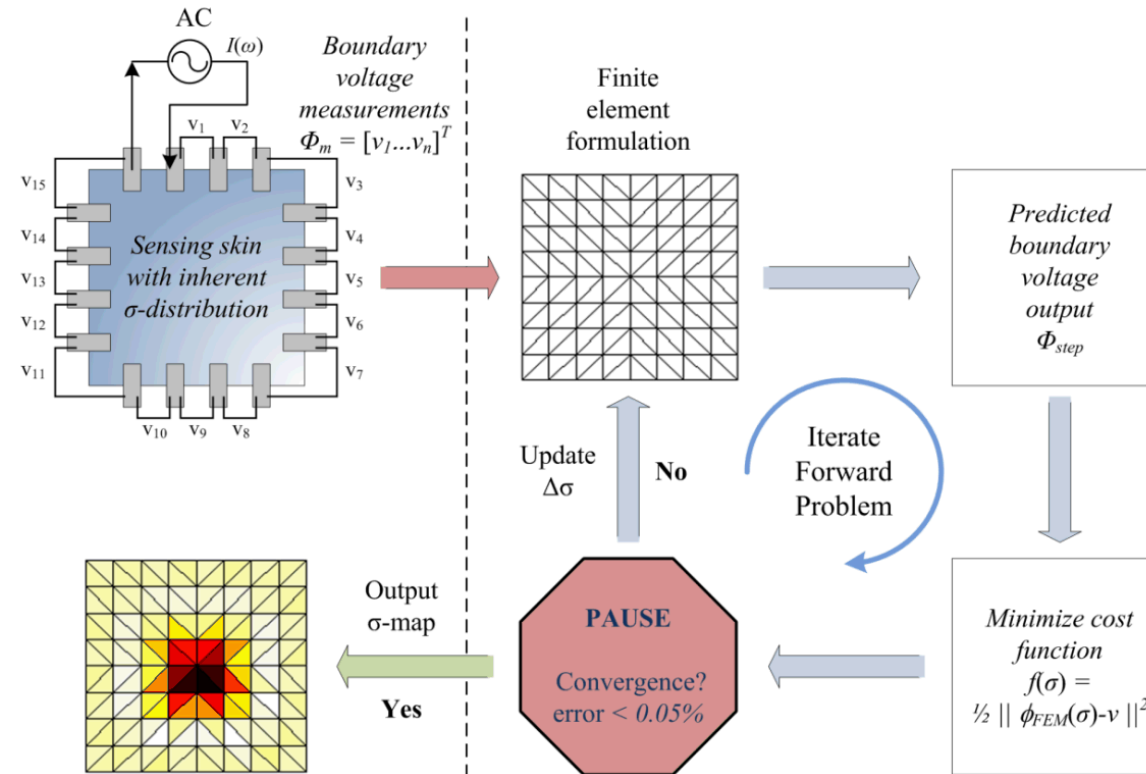
Electrical Impedance Tomography

- **Electromagnetic imaging technique**
 - ❖ Compute $\tilde{\gamma}(\omega) = \sigma + j\omega\epsilon$
- **Measure voltage response of injected current**
- **Solve conductivity**
 - ❖ Inverse problem:
 - ❖ $\min \left\{ \|V^{meas} - V^{calc}(\tilde{\gamma})\| + C(\tilde{\gamma}) \right\}$
- **Inverse problem methods**
 - ❖ Statistical-probabilistic
 - ❖ Linear Methods
 - ❖ Direct / Iterative
 - ❖ Non-linear Methods
 - ❖ Iterative



Iterative EIT Reconstruction

- **Laplace's equation:**
 - ❖ $\nabla \cdot (\sigma \nabla \phi) = 0$, where σ can vary by orders of magnitude
 - ❖ Governs potential and conductivity relationship
- **Forward problem: conductivity known, solve voltage**
- **Inverse problem: voltage known, solve conductivity**

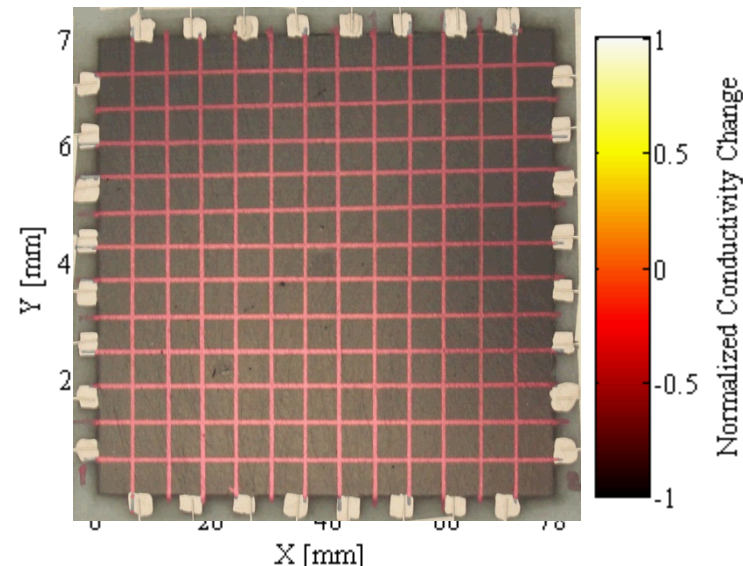


Linear EIT Reconstruction

- **Reconstructs small σ changes**
 - ❖ Typically difference imaging
 - ❖ $\sigma_1 - \sigma_2 \ll \sigma_2$
- **Maximum a posteriori (MAP)**
 - ❖ H: sensitivity matrix
 - ❖ Regularization hyperparameter: λ
 - ❖ Noise figure
 - ❖ $NF(\lambda) = \frac{SNR_{in}}{SNR_{out}} \approx 1$
 - ❖ Use representative σ distribution
 - ❖ W: Noise model
 - ❖ R: Regularization matrix
- **Advantages**
 - ❖ Can pre-calculate H
 - ❖ Many damage modes lead to small changes in σ

$$\frac{\Delta\sigma}{\sigma_0} = \left(\underline{H}^T \underline{W} \underline{H} + \underline{\lambda} \underline{R} \right)^{-1} \left(\underline{H}^T \underline{W} \right) \frac{\Delta V}{V_0}$$

$$\frac{\Delta\sigma}{\sigma_0} = B\Delta \frac{\Delta V}{V_0}$$



Validation EIT

Applied sensing measurements

- ❖ MWNT-Latex deposited upon cured GFRP composites
- ❖ 78 mm x 78 mm sensing region
- ❖ 8x8 electrodes scheme = 32 electrodes
 - ❖ 3 mm electrodes
 - ❖ 6 mm spacing

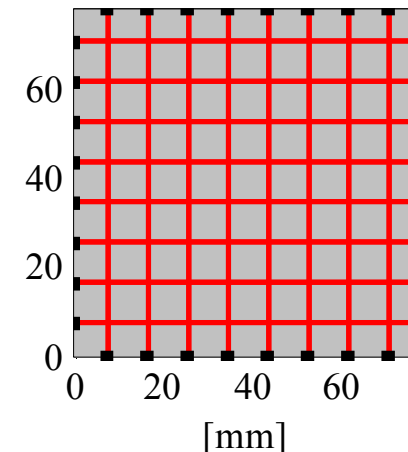
Investigate stability and efficiency:

- ❖ Computational demand
 - ❖ ~ 1 s reconstruction time

Accuracy characterization:

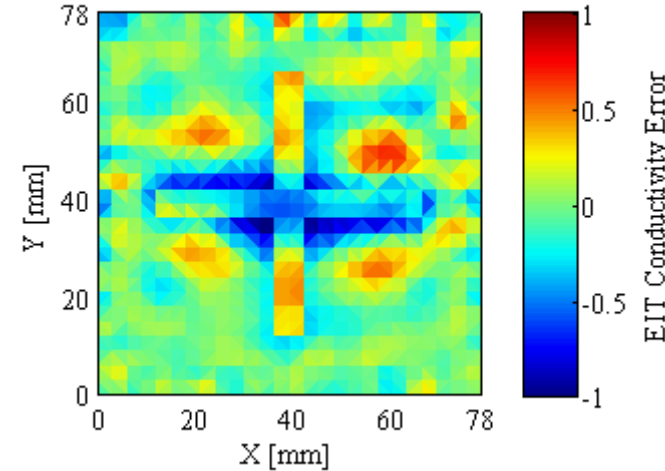
- ❖ Conductivity:
 - ❖ Point-to-point resistance map via 4-pt probe
- ❖ Spatial feature ID sensing resolution
 - ❖ ~ 6 mm square at center with -50% $\Delta\sigma$

Current Injection Pattern



[mm]

EIT Error



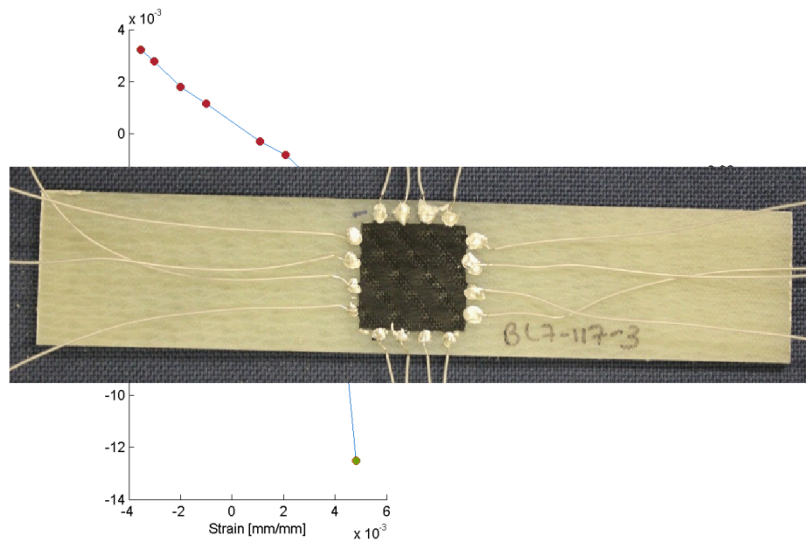
EIT Conductivity Error



Spatial Strain Sensing

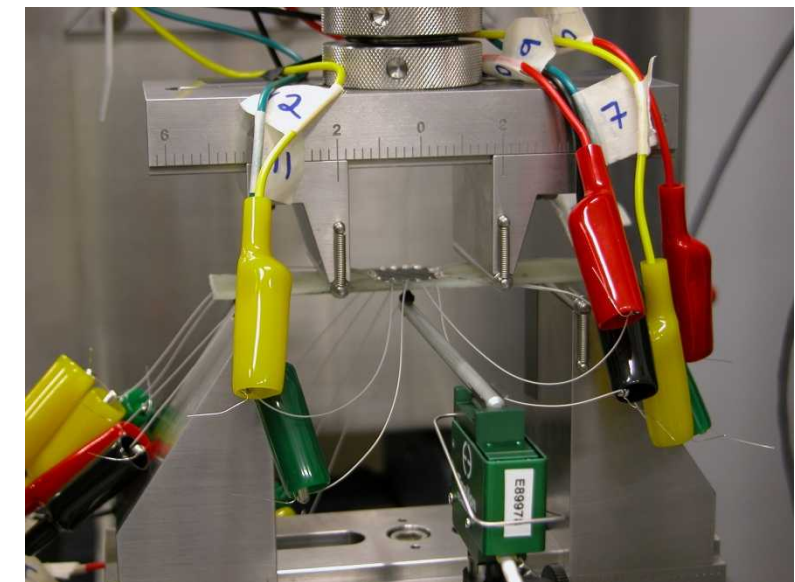
- **4-pt bending**

- ◊ ASTM D7264
- ◊ MWNT-Latex on GFRP
- ◊ Stepped displacement profile
- ◊ Tensile/compressive strains



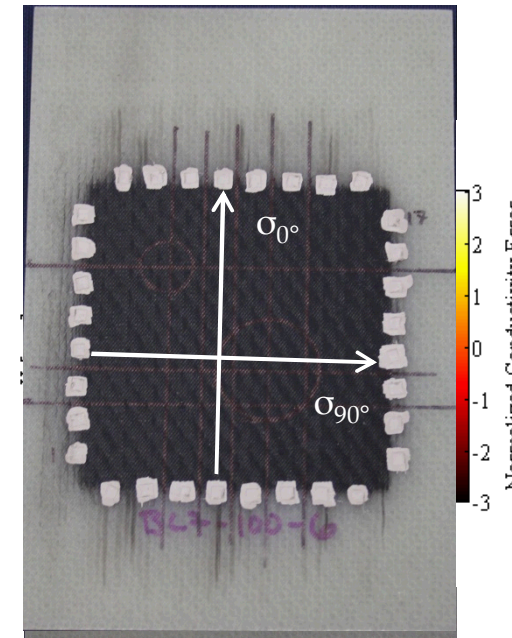
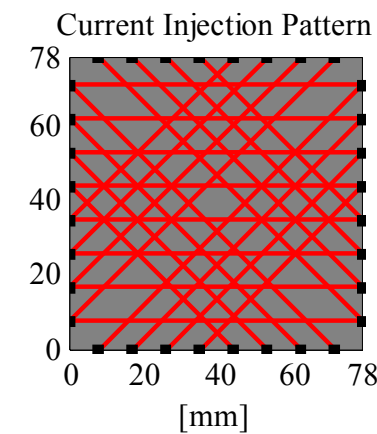
- **Strain sensitivity**

- ◊ Nearly linear



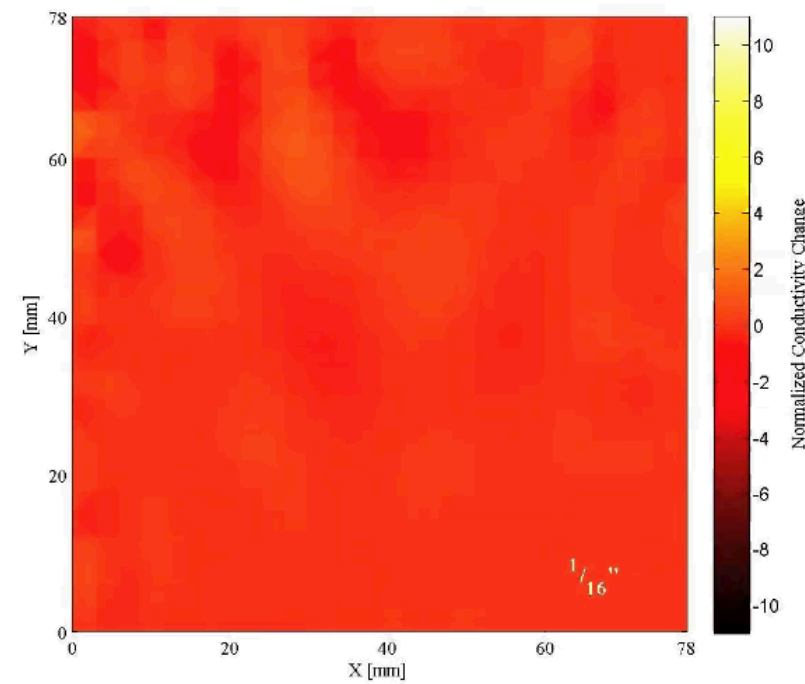
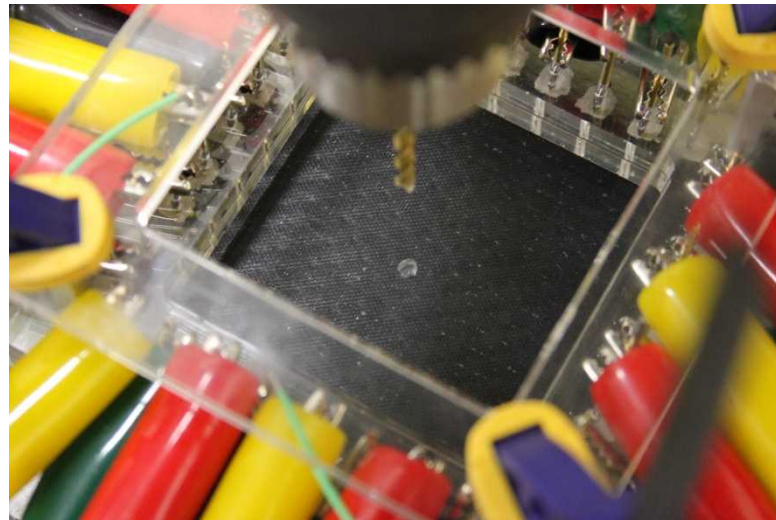
Embedded Spatial Sensing

- **Embedded sensing architecture**
 - ❖ MWNT-latex on GF fiber weave
 - ❖ Embedded within epoxy matrix
- **Specimens**
 - ❖ $[0^\circ/ +45^\circ/ 90^\circ/ -45^\circ]_{2s}$
 - ❖ Unidirectional GF
 - ❖ 150 mm x 100 mm
 - ❖ ASTM D7146 Standard
- **Anisotropic EIT**
 - ❖ Isotropic ▶ Anisotropic
 - ❖ Scalar ▶ Matrix: σ
 - ❖ $\sigma_{0^\circ} > \sigma_{90^\circ}$ by $\sim 2:1$
 - ❖ $\nabla \cdot (\sigma \nabla \phi) = 0$



Embedded Spatial Sensitivity

- **Embedded sensing validation:**
 - ❖ Determine conductivity change sensitivity
 - ❖ Process:
 - ❖ Progressively larger drilled holes:
 - ❖ $1/16''$, $1/8''$, $3/16''$, $1/4''$, $5/16''$, $3/8''$, $1/2''$
 - ❖ Anisotropic EIT performed
 - ❖ Conductivity change from pristine sample



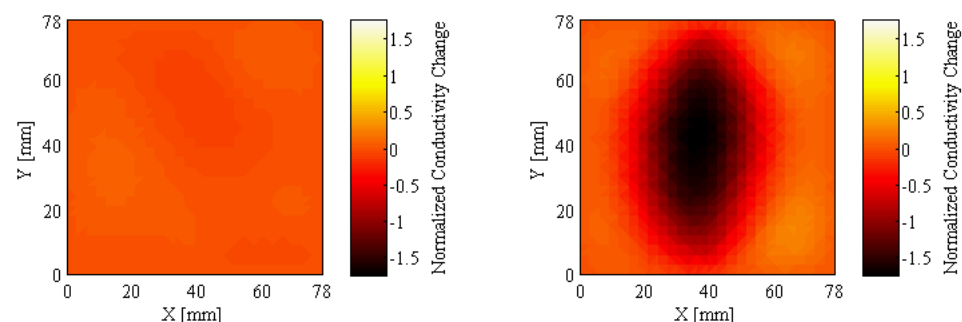
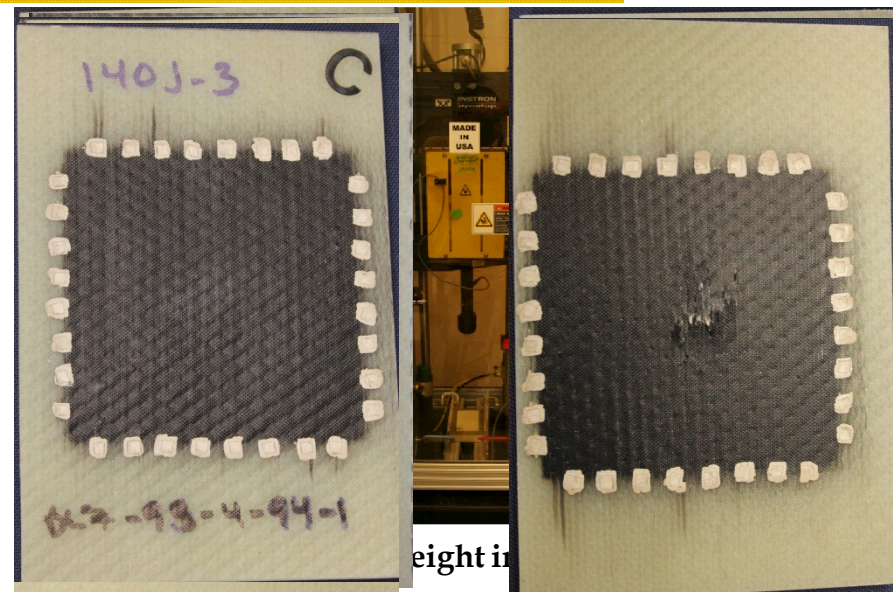
Impact Damage Detection

Drop-weight impact tests

- ASTM D7146
- 78 mm by 78 mm sensing region
- MWNT-latex on glass fiber weave
- Impact energy: 20, 60, 100, 140 J
- Before/after EIT measurements

Verification:

- Thermography
 - Matrix Cracking
 - Delamination
- Photographic Imaging
 - Surface damage



Summary

- **Propose a next-generation SHM system**
 - ❖ Direct in situ damage detection
 - ❖ Monitor location and severity of damage
- **Embedding multi-modal sensing capabilities**
 - ❖ Development of MWNT-nanocomposites for SHM
 - ❖ Characterized electromechanical response to monotonic and dynamic strain
 - ❖ Response to temperature swings
- **Outline validation of EIT for damage detection**
 - ❖ Strain sensitivity
 - ❖ Damage sensitivity
 - ❖ Impact damage





Thank You! Questions?

UNIVERSITY OF CALIFORNIA, DAVIS



Acknowledgements:

UC Davis Dissertation Year Fellowship



NINE @ Sandia National Laboratories



National Science Foundation



**Center for Information Technology
Research for the Interest of Society**



**College of Engineering,
University of California, Davis**



CFRP Sensing

- **Carbon Fiber Reinforced Polymers**
 - ❖ Highly anisotropic conductivity
 - ❖ Inhomogeneous
- **EIT Model**
 - ❖ Isotropic
 - ❖ Homogeneous
 - ❖ Gives reasonable results within bounds



Future Research Interests

□ Basic science

- ❖ Continue improving EIT reconstruction algorithms
- ❖ Investigate sensitivity mechanisms
 - ❖ Mechanical
 - ❖ Thermal
 - ❖ Chemical
- ❖ Development of new sensors
 - ❖ Nanoparticle-based
 - ❖ Electroactive polymers

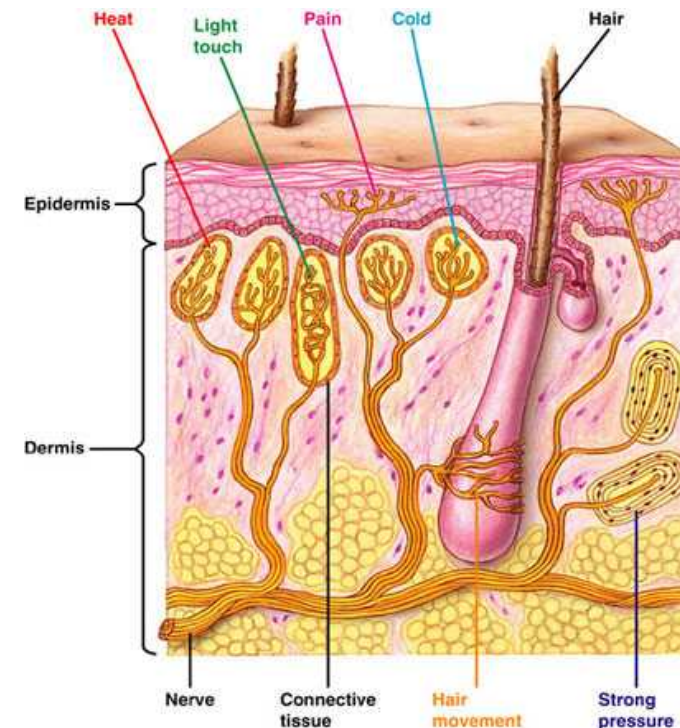
□ Application

- ❖ Extend EIT to wireless monitoring
- ❖ Implementing new EIT methods specifically designed for SHM
- ❖ Grid-based EIT



Bio-Inspired Sensing

- **Two important fundamental limitations of SHM technology:**
 1. *Indirect sensing approaches*: Sensors do not sense damage directly
 2. *Point-based sensing*: “point” sensors do not detect spatial structural behavior
- **Human dermatological system:**
 - ❖ Multifunctional material:
 - ❖ Strong to keep germs out
 - ❖ Temperature regulation
 - ❖ Absorption of nutrients
 - ❖ Sensing
- **Sensing with spatial recognition**
 - ❖ Stimulus localization
 - ❖ Multi-modal sensing:
 - ❖ Multiple receptor types
 - ❖ Intricate network of nerves



Overview of the human dermatologic system (Mallory 2008)



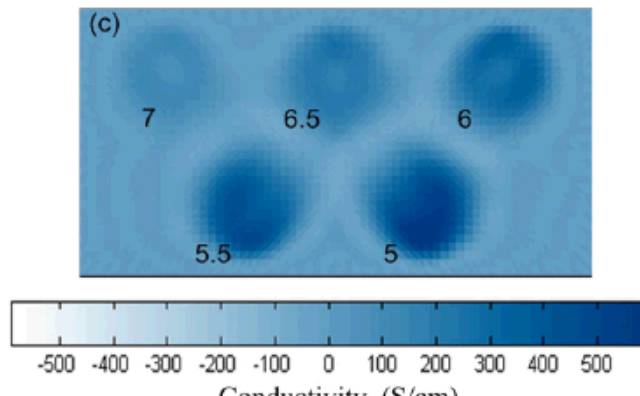
Previous Research on Spatial Sensing

□ SWNT-PE thin films

- ❖ Homogeneous substrates
 - ❖ Aluminum
 - ❖ Glass

□ Previous SHM EIT work has shown:

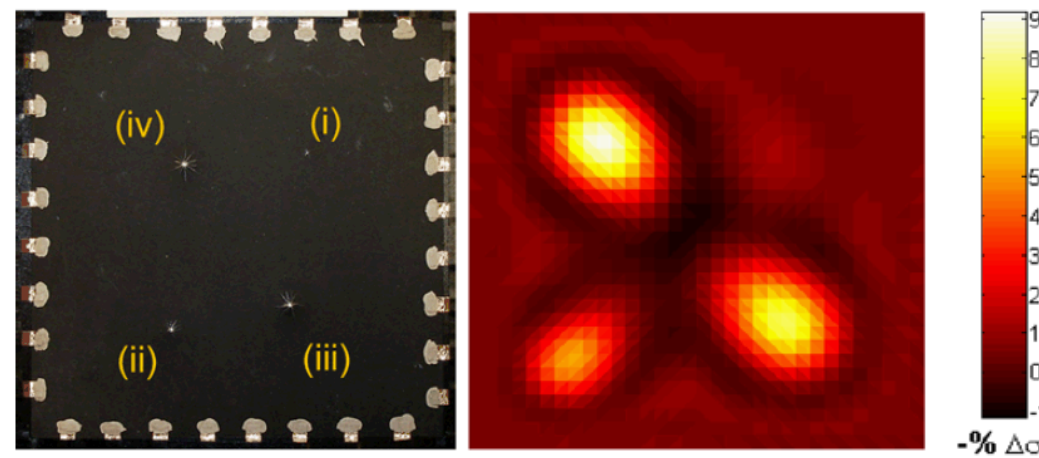
- ❖ Linear strain sensitivity
- ❖ Impact sensitivity
- ❖ pH sensitivity



pH sensitivity
Hou et al. (2009)

□ Limitation

- ❖ DC currents only
- ❖ Single current pattern
- ❖ Slow converging inverse algorithm
- ❖ Desire in situ sensing

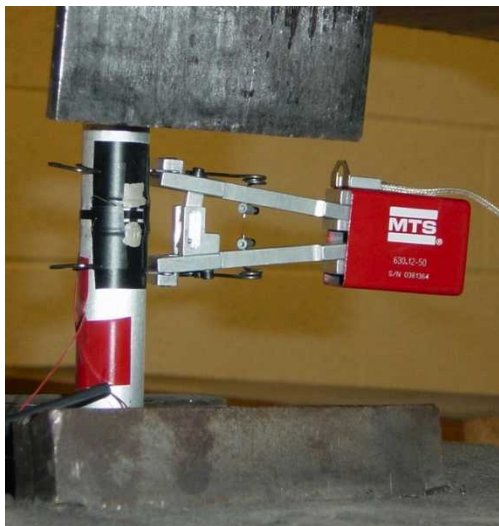


Impact damage sensitivity
Loh et al. (2009)

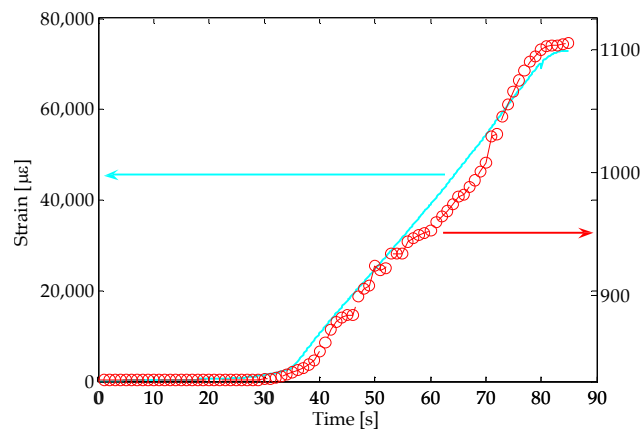


Encoding Piezoresistivity for Strain Sensing

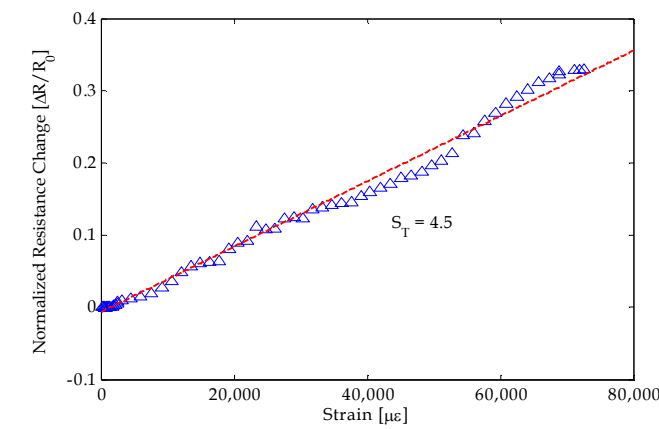
- **Piezoresistivity based on percolated SWNT nanostructure**
 - ❖ Bulk electrical conductivity influenced by number of nanotube-to-nanotube junctions
 - ❖ Applied strain modifies the number of conductive junctions
- **Monotonic tensile testing to explore thin film piezoresistivity:**



Nanocomposite monotonically loaded in tension



Resistance time history due to applied tensile strain

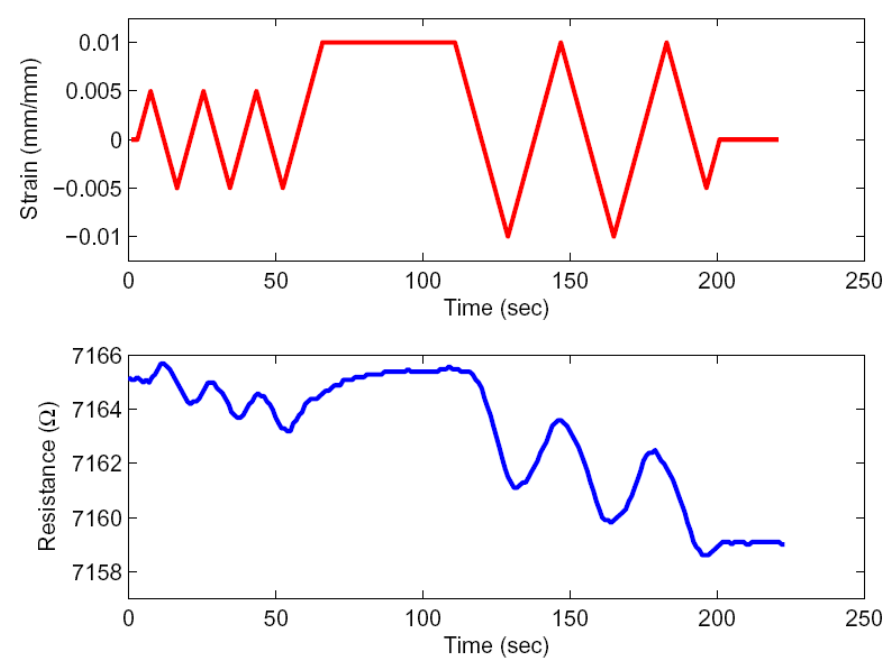
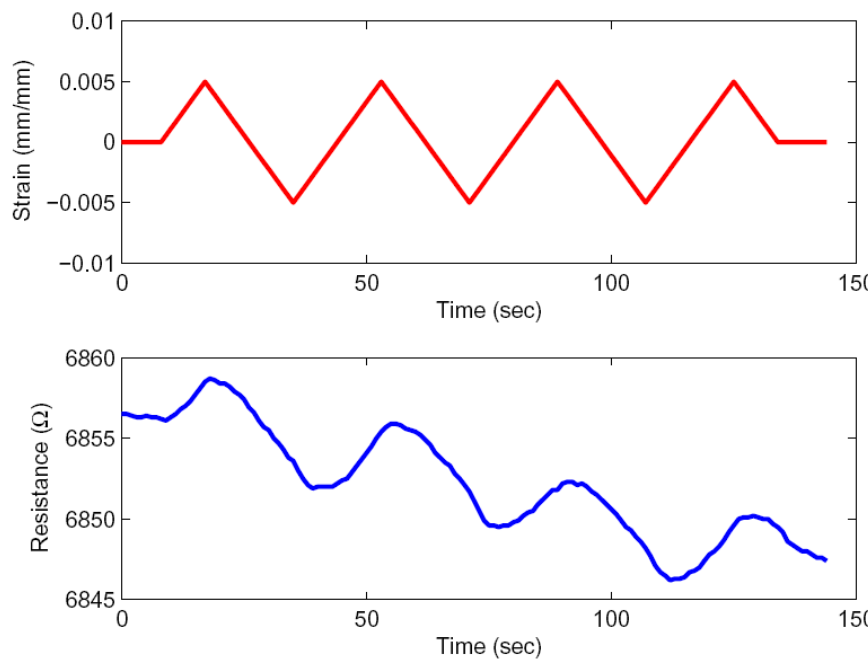


Nanocomposite piezoresistive linearity



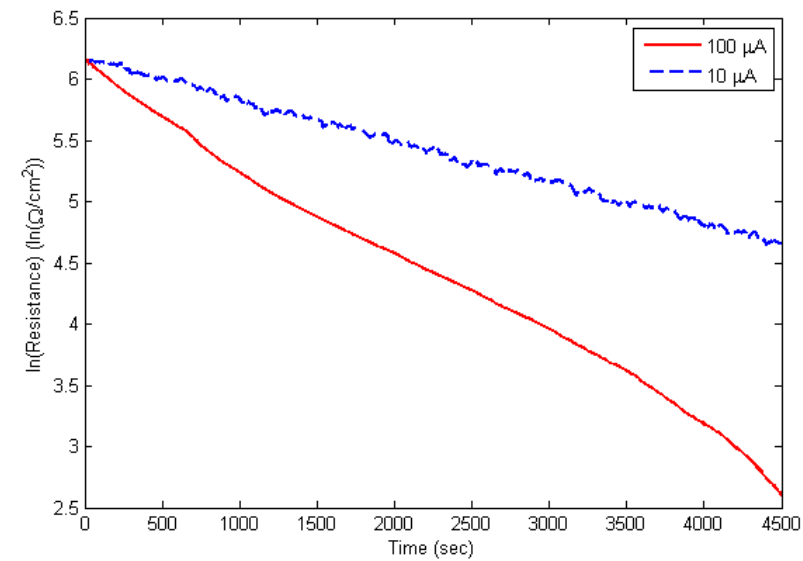
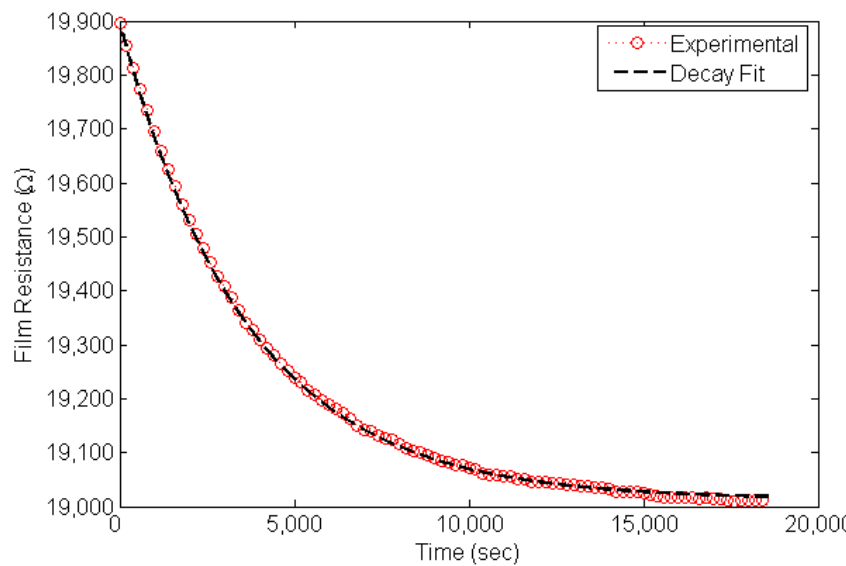
Nanocomposite Strain Sensor Response

- **Applied cyclic tensile-compressive strains ($\pm 10,000 \mu\epsilon$)**
 - ❖ Detect both tensile and compressive strains
 - ❖ Linear response beyond $10,000 \mu\epsilon$ and without film failure
 - ❖ Load-pattern and load-rate independent
- **Drawback: undesirable nominal resistivity drift**



Inherent Electrical Properties

- **Observe decay in nominal film resistivity**
 - ❖ Resistance drift not due to contact effects
 - ❖ Decay rate dependent on applied current

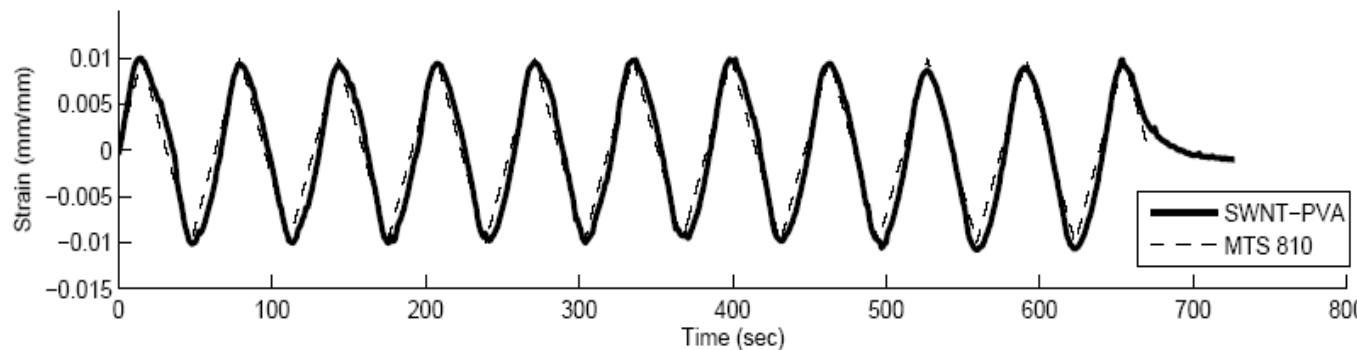


- ❖ Nominal resistivity decay may be due to localized heating and physical/chemical changes in nanotube composite
- ❖ Decay can be modeled accurately $\rightarrow R = A e^{-Bt} + C$

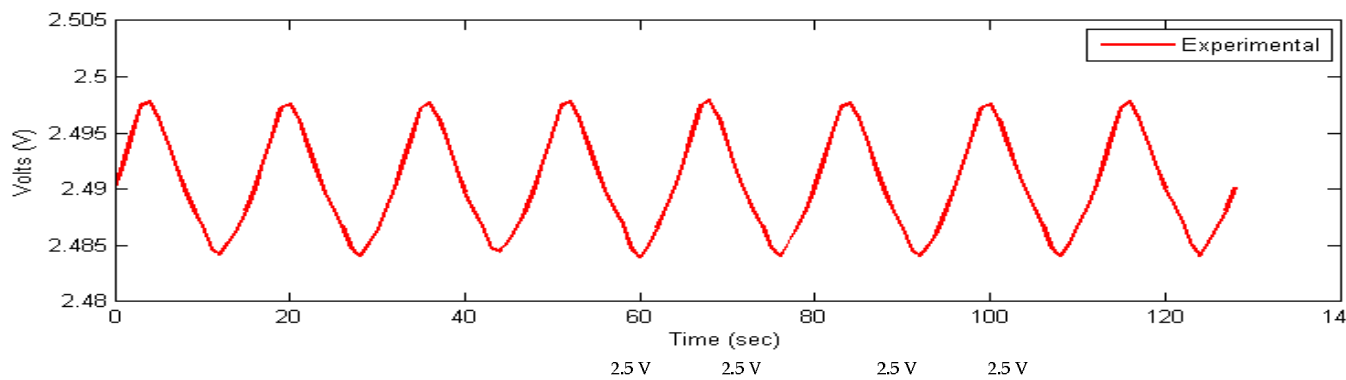


Drift-free Strain Sensing Response

- Exponential drift can be numerically removed to obtain drift-free response:



- High-pass filtering can be employed for dynamic strain measurements:

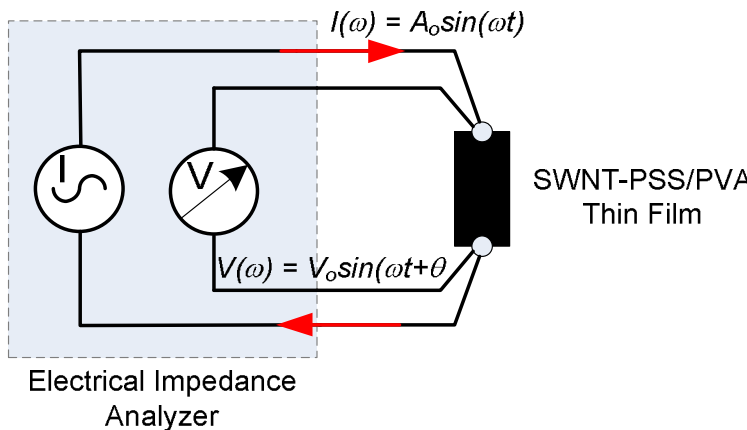


- Disadvantageous for structural health monitoring in field environments

Passive and Active SHM Strategy

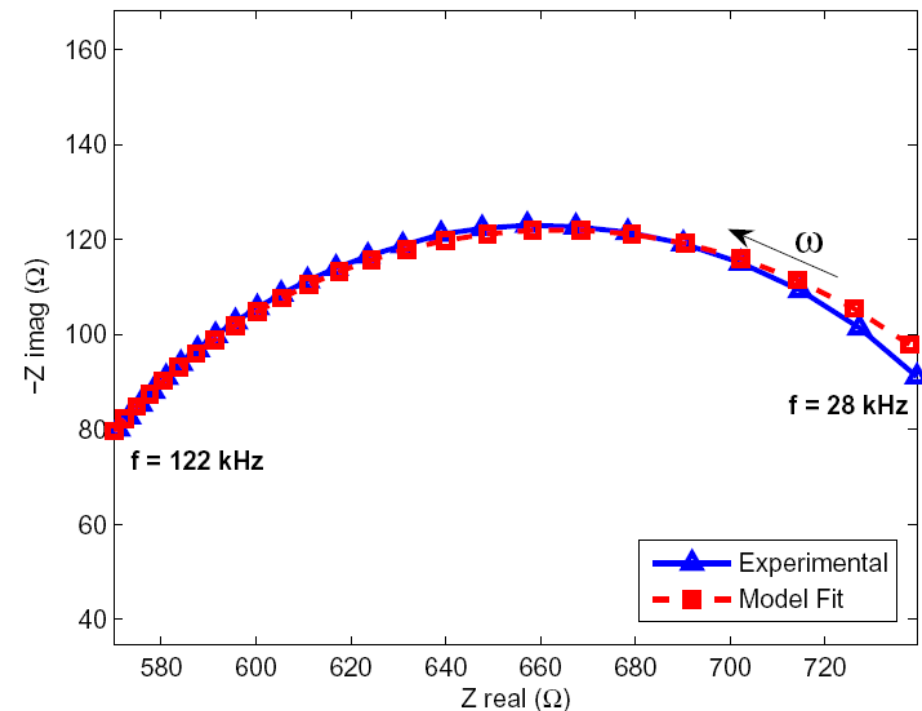


Electrical Impedance Spectroscopy (EIS)



$$Z = \text{Re}(Z) + \text{Im}(Z)j$$

$$\text{Re}(Z) = \left| \frac{V_o}{I_o} \right| \quad \text{Im}(Z) = \theta$$



- Characterize SWNT-PSS/PVA thin film electrical properties:
 - Measured impedance using regulated electrical current signals (AC: 25 – 125 kHz)
 - Cole-Cole (or Nyquist) plots of complex impedance reveal thin film electrical properties
 - Formulate equivalent circuit model to describe strain and nominal resistance drift



Enhanced Thin Film Mechanical Properties

- As-fabricated LbL films show good mechanical performance compared to other composites
 - Mechanical properties important for long-term SHM applications
 - Significant mechanical performance improvements compared to buckypaper

	Buckypaper ¹ (Blighe, <i>et al.</i> 2008)	Epoxy-Resin ² (Gojny, <i>et al.</i> , 2004)	Layer-by-Layer ¹ (Loh, <i>et al.</i> 2010)
Young's modulus, E	1.3 GPa	3.3 GPa	13.0 GPa
Ultimate tensile strength, σ_f	7.5 MPa	63 MPa	215 MPa
Ultimate failure strain, ε_f	5,000 $\mu\epsilon$	68,000 $\mu\epsilon$	58,300 $\mu\epsilon$

¹ Based on single-walled carbon nanotubes (SWNTs)

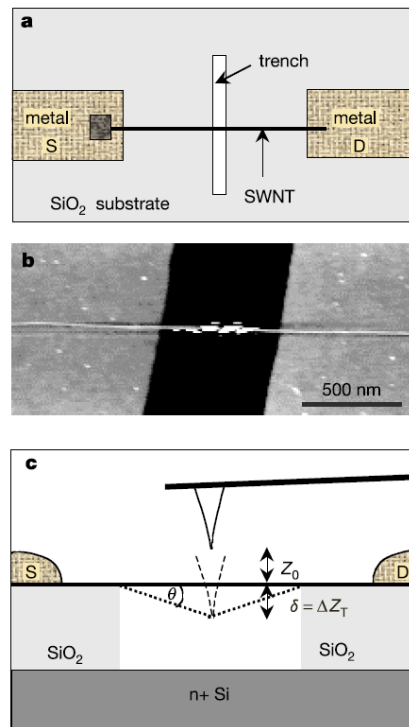
² Based on double-walled carbon nanotubes (DWNTs)

- Seek to further enhance mechanical and fracture performance:
 - Post-fabrication thermal annealing → polymer cross-linking
 - Optimize carbon nanotube weight content



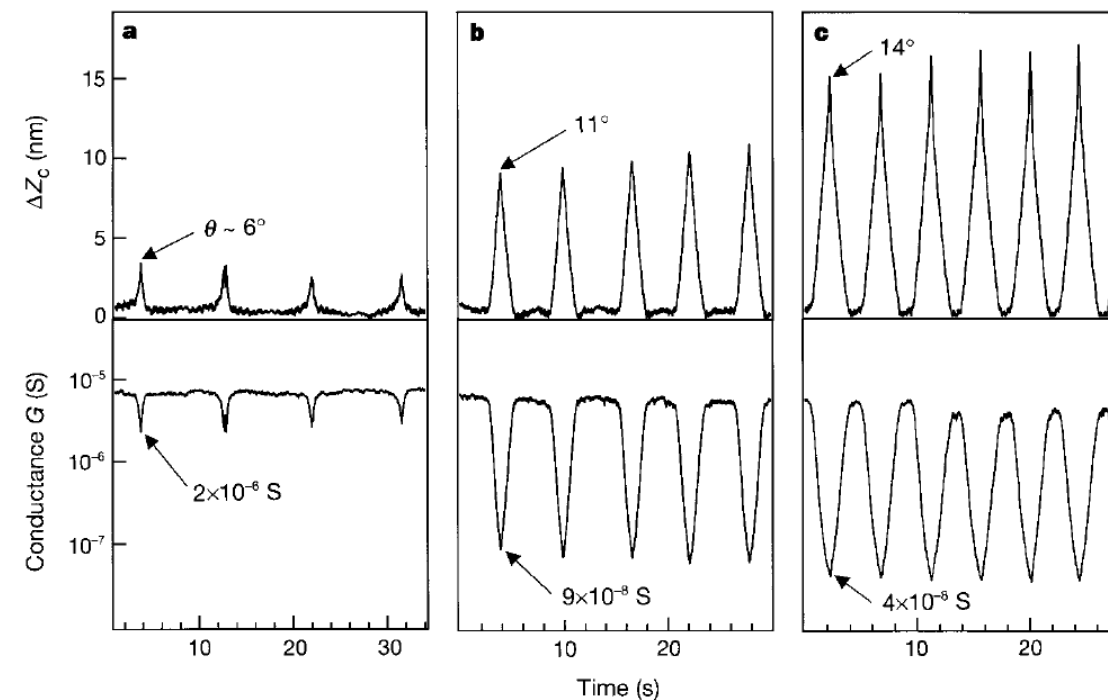
Nano-Scale Sensing Performance

- **Early experimental studies on carbon nanotube strain sensing performance conducted with atomic force microscope (AFM)**
 - ❖ Use tip to bend individually-suspended SWNTs
 - ❖ At 3% strain, conductance decreased by more than two orders of magnitude



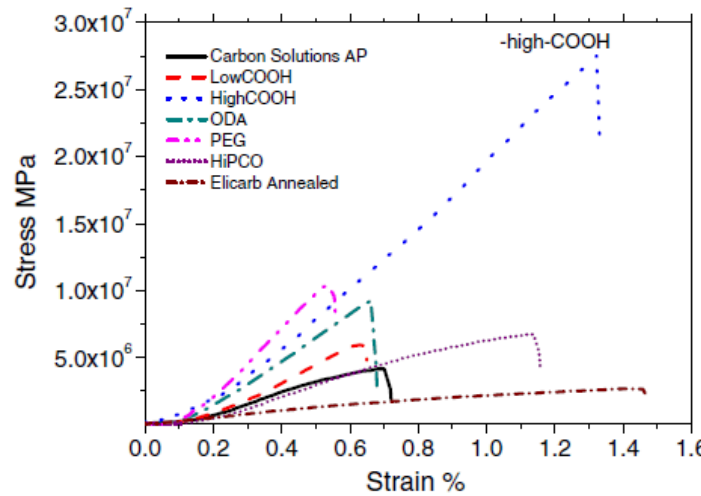
Individual SWNT suspended over trench

Applied AFM tip deflection and measured conductance
(Tombler, *et al.*, 2000) Stanford University

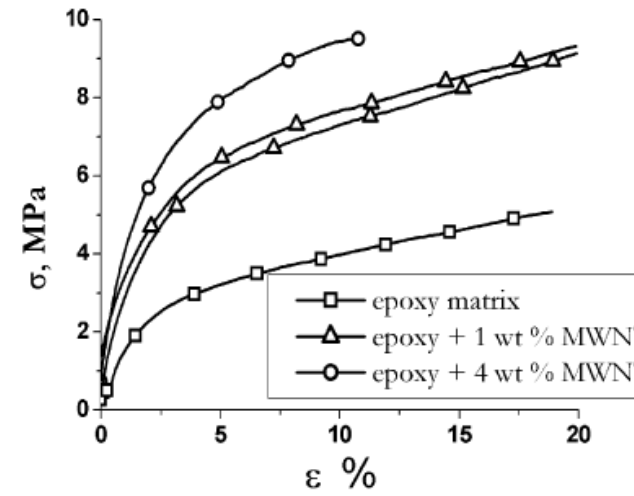


Limitations of Current Nanocomposites

- **Current-generation composites employ mixing of multiple ingredients:**
 - ❖ Carbon nanotubes with polystyrene
 - ❖ Carbon nanotubes in epoxy-resin
- **Employs traditional composite design methodology to optimize one material property**
 - ❖ Buckypaper – high stiffness, but low ductility and ultimate tensile strength



Buckypaper stress-strain responses
(Blighe, *et al.*, 2008) Trinity College of Dublin

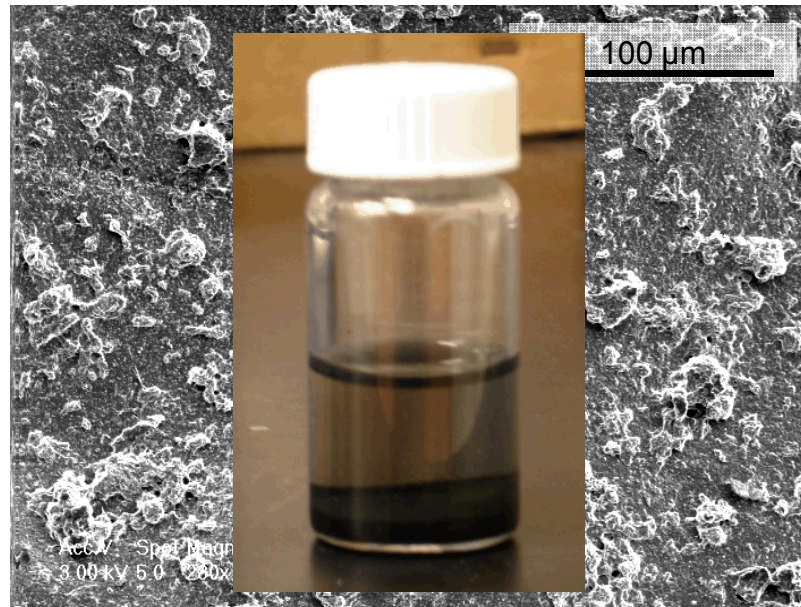


Epoxy-resin stress-strain responses
(Allaoui, *et al.*, 2002) Shenyang National Lab

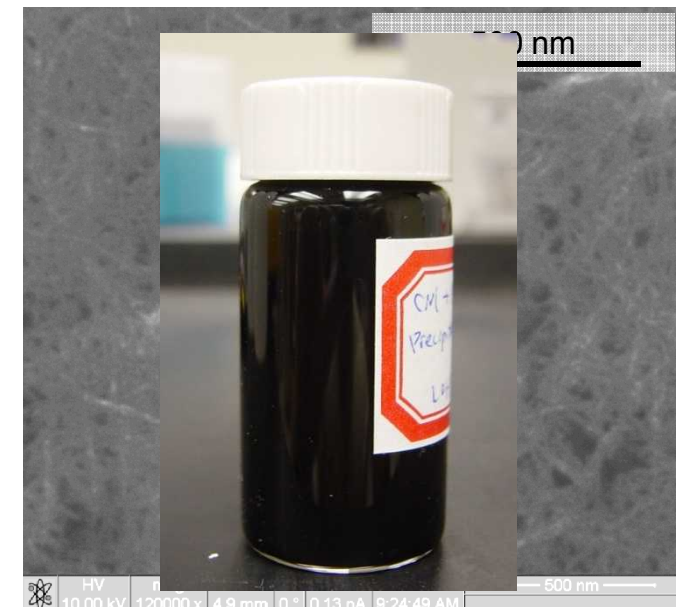


Challenges with Using Carbon Nanotubes

- **Difficult to scale nanomaterial properties to the macro-scale:**
 - ❖ Tendency to agglomerate due to strong van der Waals interactions
 - ❖ Leads to poor material properties in buckypaper specimens



Poorly-dispersed SWNT solution



Well-dispersed SWNT-PSS solution

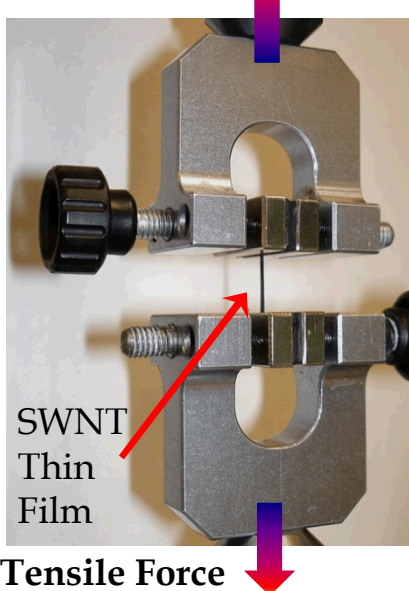
Scanning electron microscopic (SEM) views of carbon nanotube thin films



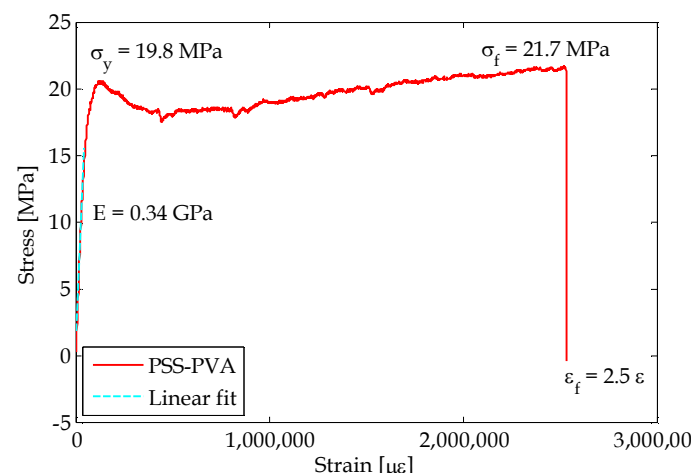
LbL Nanocomposite Mechanical Properties

- Morphology consists of mechanically-strong and -stiff nanotubes sitting in a highly compliant polymeric matrix
 - Dramatic improvements in nanocomposite strength and stiffness
 - SWNT-tuned composites exhibit high ductility ($> 10,000 \mu\epsilon$)

Tensile Force

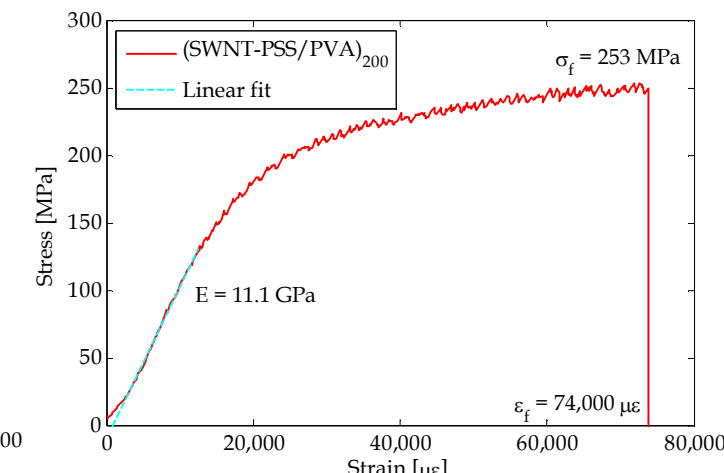


Tensile Force



Nanocomposite strained

PSS/PVA polymeric
nanocomposite



Carbon nanotube-reinforced SWNT-
PSS/PVA LbL composite



Enhanced Thin Film Mechanical Properties

- As-fabricated LbL films show good mechanical performance compared to other composites
 - Mechanical properties important for long-term SHM applications
 - Significant mechanical performance improvements compared to buckypaper

	Buckypaper ¹ (Blighe, <i>et al.</i> 2008)	Epoxy-Resin ² (Gojny, <i>et al.</i> , 2004)	Layer-by-Layer ¹ (Loh, <i>et al.</i> 2008)
Young's modulus, E	1.3 GPa	3.3 GPa	11.1 GPa
Ultimate tensile strength, σ_f	7.5 MPa	63 MPa	253 MPa
Ultimate failure strain, ε_f	5,000 $\mu\epsilon$	68,000 $\mu\epsilon$	74,000 $\mu\epsilon$

¹ Based on single-walled carbon nanotubes (SWNTs)

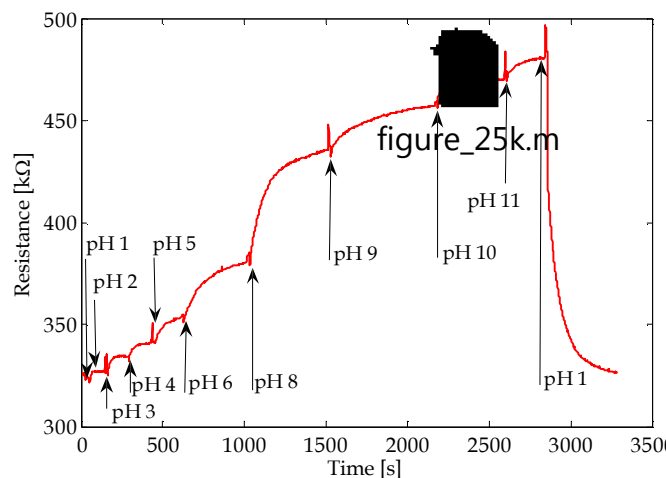
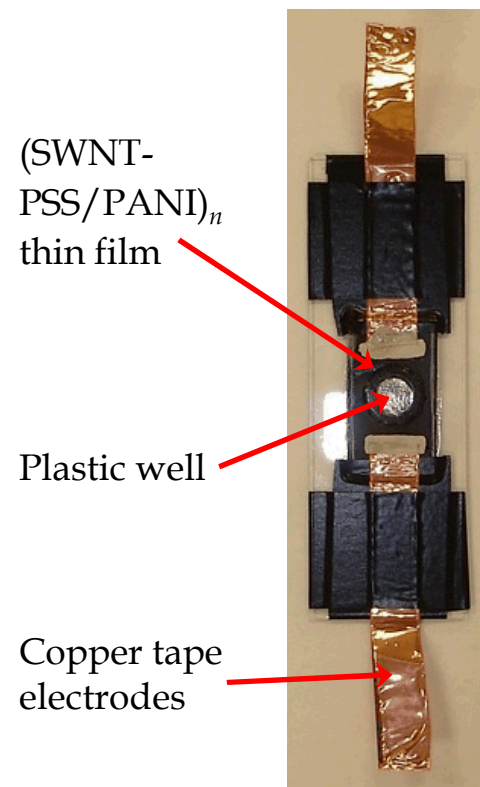
² Based on double-walled carbon nanotubes (DWNTs)

- Quasi-static load tests only reveal time-independent mechanical response:
 - Layer-by-layer films are polymer-based nanocomposites
 - It is likely that they exhibit time-dependent mechanical properties such as viscoelasticity

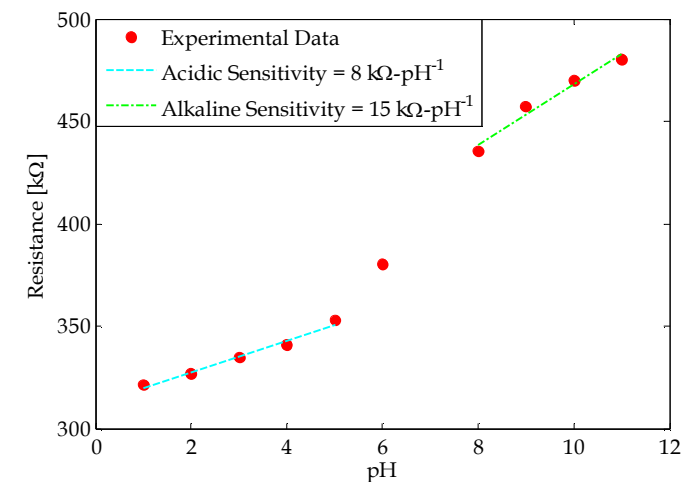


Nanocomposite pH Sensing

- **LbL versatility allows us to encode pH sensitivity within thin films:**
 - ❖ Can be used for monitoring corrosion or biological processes
 - ❖ Employ pH-sensitive polyelectrolyte: poly(aniline) emeraldine base (PANI)



Resistance time history due to pH variations



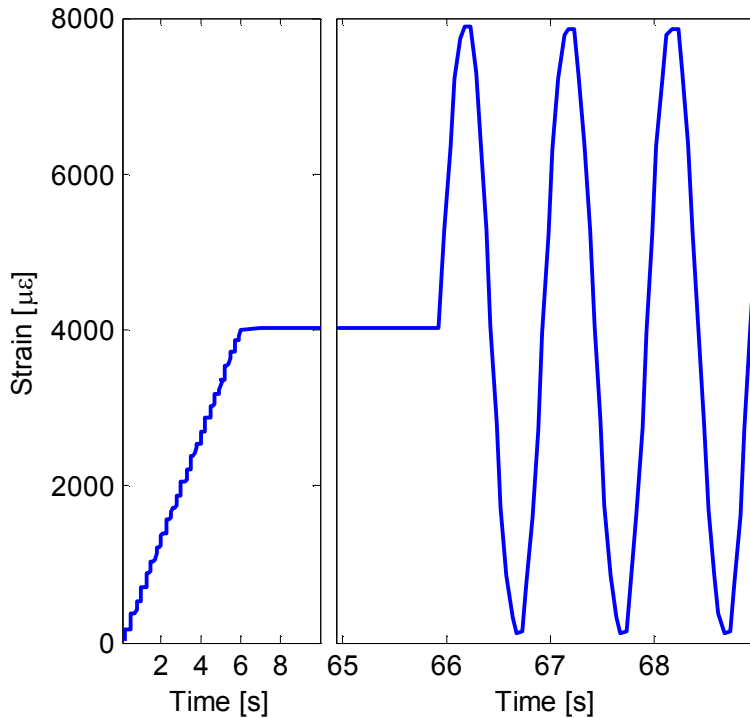
Nanocomposite pH sensitivity



Fatigue Sensor Characterization

- Long-term low strain dynamic response

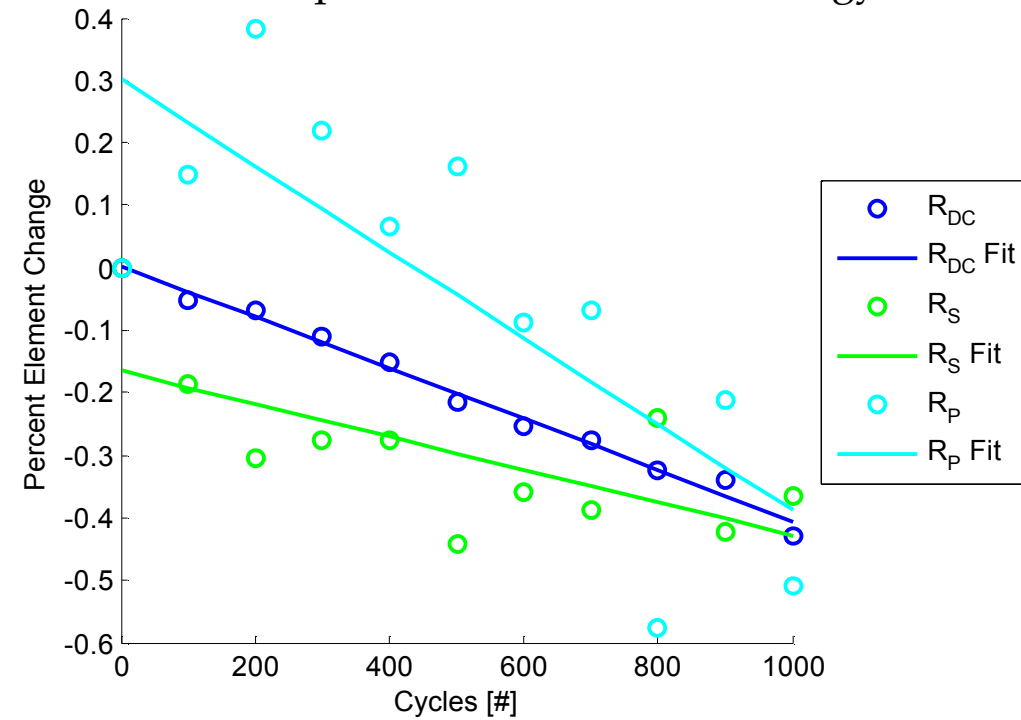
- Off-set: $+4,000 \mu\epsilon$
- Amplitude: $4,000 \mu\epsilon$



Applied strain profile

- Long-term dynamic response:

- Slight linear trend in response
- Less than 0.5% over 1,000 cycles
- Demonstrates the robust sensing capabilities of this methodology

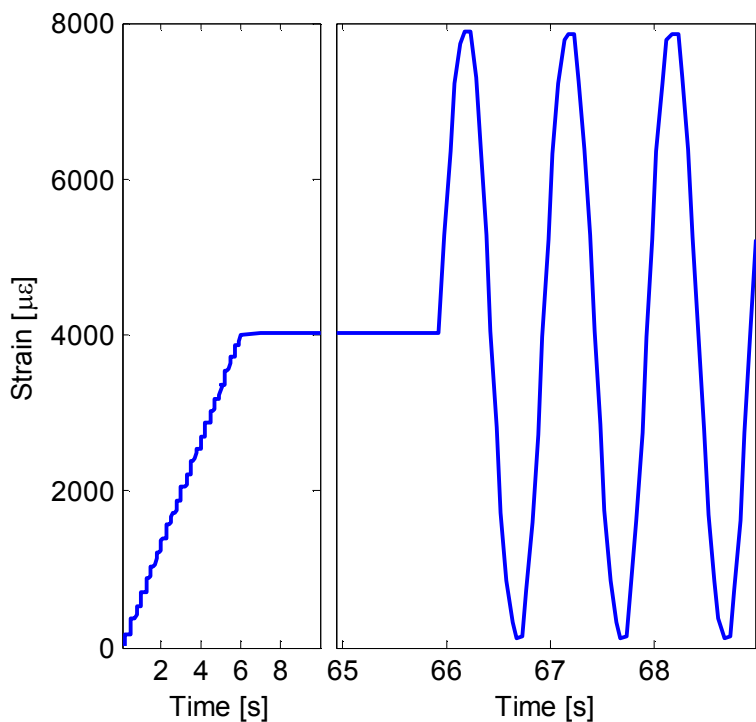


Applied strain profile

Fatigue Sensor Characterization

- **Long-term low strain dynamic response**

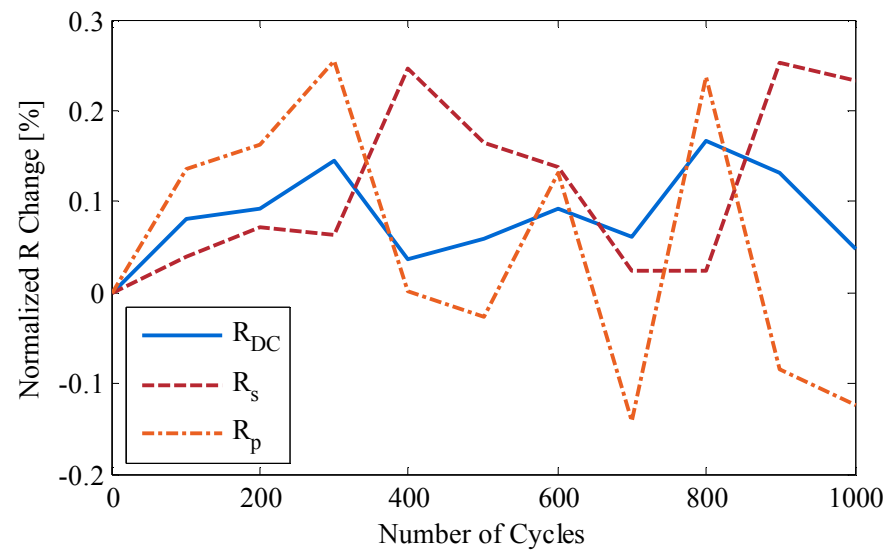
- Off-set: $+4,000 \mu\epsilon$
- Amplitude: $4,000 \mu\epsilon$



Applied strain profile

- **Long-term dynamic response:**

- Slight linear decrease in response
- Less than 0.5% over 1,000 cycles
- Demonstrates the robust sensing capabilities of this methodology



Applied strain profile

